

1 **Simulating recent warming of the Great Lakes in an idealized lake–ice–atmosphere model**

2

3

by

4

5

Noriyuki Sugiyama, Sergey Kravtsov¹ and Paul Roebber

6

7

University of Wisconsin-Milwaukee

8

9

10

27 February 2017

11

12

Submitted to the *Journal of Climate*

13

14

15

16

17

18

19

20

21

¹*Corresponding author address:* Dept. of Mathematical Sciences, Atmospheric Science Group,
University of Wisconsin-Milwaukee, P. O. Box 413, Milwaukee, WI 53201. *E-mail:*
kravtsov@uwm.edu.

1 **Abstract**

2 The Laurentian Great Lakes recently exhibited summertime surface warming whose rate
3 substantially exceeded those of the overlying atmosphere and surrounding areas. This warming
4 had a jump-like character, switching from a regime of preferred cold seasonal cycles with
5 extensive ice coverage and low summertime temperatures characterizing the 1988–1997 period,
6 to the one dominated by warm seasonal cycles of little-to-no ice and extreme summertime
7 warmth in the 1998–2007 period. The dynamics of this phenomenon are examined here using an
8 idealized coupled lake–ice–atmosphere model driven by the observed history of the external
9 large-scale forcing. The model version of Lake Superior captures well both the 1997/98
10 transition to a warm climate regime, as well as the observed decadal persistence of the cold and
11 warm states on either side of this transition. By contrast, the same model, but with the ice–albedo
12 feedback artificially suppressed, is only able to capture about 60% of the observed warming, due
13 to a warm bias in its simulations of the cold 1988–1997 period. It is demonstrated that
14 nonlinearity associated with the ice–albedo feedback, and the resulting persistence of the
15 simulated cold regime, is central in rationalizing the observed characteristics of the Great Lakes’
16 warming. The ice–albedo feedback is estimated to be directly responsible for about 30–40% of
17 the observed summertime warming over the eastern Lake Superior, with the remainder forced by
18 long-term changes in the external large-scale conditions, possibly augmented by other local
19 feedbacks not explicitly represented in the present model.

20

21

22

23

1 **1. Introduction**

2 Rapid summertime surface warming of mid-latitude lakes in recent decades, with rates
3 exceeding those of the surrounding land's warming by a factor of two or more, is a ubiquitous
4 phenomenon that drew much scientific attention (Schneider and Hook 2010; O'Reilly et al.
5 2015). The reasons as to why some of the lakes exhibit accelerated warming and some don't, as
6 well as the mechanisms behind the lacustrine amplification of large-scale warming are still a
7 subject of active debate. Possible scenarios include increases in downward shortwave radiation
8 and air temperature (Arvola et al. 2010; Fink et al. 2014; Gronewold et al. 2015), shorter ice
9 season (Magnuson 2000), as well as earlier onset of the summertime stratification (Austin and
10 Colman 2007; Austin and Allen 2011; Piccolroaz et al. 2015; Zhong et al. 2016). An emerging
11 view is that the dominant dynamics of the accelerated lake warming depend on a region
12 (O'Reilly et al. 2015). For example, a large-scale decrease in cloud cover over the United States
13 may have been the primary physical driver of the lake warming in California and Nevada
14 (Schneider et al. 2009).

15 The focus of the present paper is on the Great Lakes, which, incidentally, exhibited a great
16 variety of decadal warming rates among its individual constituents, pointing to the importance of
17 internal lake dynamics in the accelerated lake warming. The deepest Lake Superior underwent
18 the most dramatic surface warming (Austin and Colman 2007), whereas the warming trends of
19 the shallowest Lake Erie did not exceed much those of the surrounding land. This relationship
20 between lake depth and surface warming trends — which is one of the striking properties of the
21 Great Lakes' recent warming — also holds within its individual lakes, with deeper regions
22 exhibiting stronger surface-warming rates (Zhong et al. 2016; Sugiyama et al. 2017).

1 The second striking aspect of the Great Lakes' surface warming is the apparent negative
2 correlation between their wintertime ice coverage and surface temperature in the following
3 summer (Hanrahan et al. 2010): the more ice covers the lakes in winter, the cooler is the
4 maximum surface temperature the lakes achieve in summer. Accordingly, the decadal warming
5 of the Great Lakes was accompanied by dramatically reduced ice coverage. Austin and Colman
6 (2007) hypothesized that the observed reduced ice coverage is at the heart of the accelerated lake
7 warming, with the associated ice–albedo feedback explaining the faster warming rates: here, the
8 heat for an extra warming would come via the increased amounts of shortwave radiation the lake
9 climate system received as the ice cover retreated.

10 Recent simulations of Zhong et al. (2016) using a regional coupled climate model challenged
11 this view, as their results were largely insensitive to the value of the ice albedo used in the
12 model. These authors argued instead that the observed correlation between the lake ice and
13 summertime surface temperatures was not causal, but reflected the lake response to a common
14 driver associated with the wintertime climate conditions, which affected the summertime
15 temperatures by shifting the date of the lake's summertime mixed-layer formation. In this
16 interpretation, the action of the ice–albedo feedback would be negated by the inhibited heat loss
17 from the lake due to insulating lake-ice properties, with the negligible net effect on lake
18 temperature (Vavrus et al. 1996).

19 The third essential feature of the recent surface warming of the Great Lakes is its step-like,
20 rather than continuous character, indicating a persistent shift of the regional climate regime (Van
21 Cleave et al. 2014; Gronewold et al. 2015; Zhong et al. 2016). The shift was arguably instigated
22 by the strong 1997/98 El Niño event and led to the switch from pre-1998 lake-climate conditions
23 characterized preferentially by massive wintertime ice cover and cool summertime temperatures

1 to the state in which the warm regime with little-to-no-ice prevailed (compare this with the Great
2 Lakes “ice–cover regimes” introduced by Assel et al. 2003). Once again, the climate shift is most
3 noticeable in the climatic records associated with deep lakes, and is less apparent in the shallow
4 lakes. The regional climate shift above may have been related to a larger-scale climate shift
5 (Mukhin et al. 2015) manifested, among other things, in the flipped phase of the Pacific Decadal
6 Oscillation (Mantua et al. 1997). This large-scale climate change provided a persistently different
7 forcing environment for the Great Lakes in the post-1998 era, which was able, in turn, to
8 maintain a persistent change of the Great Lake’s regional climate regime. Zhong et al.’s (2016)
9 regional climate model simulations rationalized a major fraction of the Lake Superior’s warming
10 associated with the 1997/98 warming episode; however, they were only able to account for less
11 than a half of this lake’s observed summertime *decadal* warming, leaving the remainder
12 unexplained.

13 In this paper, we investigate the dynamics of the accelerated warming of the Great Lakes
14 using an idealized coupled lake–ice–atmosphere model. This model, developed in Sugiyama et
15 al. (2017), exhibits multiple regional climate regimes as distinct stable seasonal cycles of the
16 lakes that can occur under the *identical* seasonally varying forcing. These regimes dynamically
17 arise due to nonlinearity associated with the ice–albedo feedback, and are absent from the model
18 in which the ice–albedo feedback is artificially suppressed. The main point of the paper is that
19 such nonlinear regime dynamics can rationalize the decadal persistence of the cold 1982–1997
20 climate state, as well as the full magnitude of the recent observed warming of the Great Lakes,
21 thus spotlighting again the ice–albedo feedback as the major dynamical cause of the lacustrine
22 amplification of large-scale climate warming.

23

1 **2. Coupled lake–ice–atmosphere model**

2 *a. Model formulation*

3 In this study, we utilized a modified version of the thermodynamic lake/lake-ice–atmosphere–
4 land coupled model described in Sugiyama et al. (2017); the model geometry is shown in **Fig. 1**.
5 The lake component of the model has three distinct columns of different depths, which do not
6 directly exchange heat with one another. The temperature distribution in each column is
7 governed by an eddy diffusion 1-D model of Hostetler and Bartlein (1990), whose vertical
8 mixing scheme is modified to ensure correct simulation of the lake’s seasonal cycle (see
9 Sugiyama et al. 2017). The ice model formulation is also thermodynamic, based on a simplified
10 1-D model of Semtner (1976). The energy-balance atmosphere on top of the lake and land areas
11 has two vertically stacked layers: the atmospheric boundary layer and the free atmosphere. The
12 evolution of the free-atmosphere temperature $T_{a,u}(t)$ is prescribed to mimic the observed
13 evolution, and acts as a forcing, along with the prescribed time-dependent downwelling
14 shortwave radiation $SW(t)$. We also prescribe the seasonally varying surface wind speed $u(t)$
15 and relative humidity $r(t)$, which enter the bulk-formula expression for the heat exchange
16 between lake/ice and the overlying atmosphere. The atmospheric boundary layer, on the other
17 hand, is interactive, and is affected by both lake/land below and the free atmosphere above. We
18 separate the atmospheric boundary layer into four sections whose boundaries coincide with those
19 of the lake columns and the land. Adjacent sections of the boundary layer exchange heat
20 horizontally via diffusive transports; they are also affected by parameterized advective transport
21 from the upwind regions (see below).

22 We considered three lakes of different bathymetry (**Table 1**). Lakes 1A and 1B are both
23 deep lakes mimicking different parts of Lake Superior; in particular, they differ by the relative

1 areas of their deep and shallow regions. Lake 2 is a shallow lake loosely corresponding to Lake
2 Erie. Accordingly, the $T_{a,u}(t)$, $SW(t)$, $u(t)$ and $r(t)$ over deep lakes are chosen based on
3 observations over Lake Superior, and those over the shallow lake — based on observations over
4 Lake Erie (see section 2b).

5 The Sugiyama et al. (2017) model above is further modified, in the present paper, to include a
6 parameterization of upwind air advection (Fig. 1), by adding, to the atmospheric boundary layer
7 equations, an extra source term of the form

$$8 \quad F_{a,i} = (\alpha c_a H_a u / \sqrt{A_l}) \times (T_{wind} - T_{a,i}). \quad (1)$$

10
11 Here $F_{a,i}$ is the advective heat flux to the i -th column of the boundary layer (whose temperature
12 is $T_{a,i}$), c_a is the volumetric heat capacity of air, H_a is the height of the atmospheric boundary
13 layer, $u(t)$ is the wind speed, and A_l is the total area of the lake. The quantity T_{wind} is the air
14 temperature upwind of the lake, which acts as the fifth prescribed (time-dependent) forcing
15 parameter, chosen based on the observations upwind of Lake Superior for Lake 1 models, and
16 upwind of Lake Erie for the Lake 2 model (see section 2b). The adjustable parameter α governs
17 the efficiency of the advective heat transport (1).

18 In addition to α , two other important adjustable parameters in our models are C_E and R . The
19 parameter C_E governs the efficiency of horizontal heat diffusion between the adjacent
20 atmospheric columns and is the same as in Sugiyama et al. (2017). The parameter R is the ratio
21 of the surface area of the surrounding land to that of the lake.

22

1 *b. Model tuning and choices of adjustable parameters*

2 We specified $T_{a,u}(t)$, $SW(t)$, $u(t)$, $r(t)$ and $T_{wind}(t)$ time series based on the North
3 American Regional Reanalysis (NARR: <https://www.esrl.noaa.gov/psd/data/gridded/data.narr.html>).
4 All of these quantities except for wind speed were derived from monthly data, with cubic-spline
5 interpolation to higher temporal resolution; the 10-m-level wind speeds were derived directly
6 from the 3-hourly data.

7 The free-atmosphere temperature time series $T_{a,u}(t)$ was based on observations of 850-mb
8 atmospheric temperature. The eastern part of Lake Superior, especially the area near and south of
9 buoy station 45004 (47.59°N, 86.59°W), is the region of the most dramatic surface-warming
10 trend among Great Lakes; hereafter, the *eastern Lake Superior* region. To emulate the forcing
11 environment corresponding to these conditions in our Lake 1 models, we used the observed
12 $T_{a,u}(t)$, $SW(t)$, $u(t)$ and $r(t)$ at this station's location. For Lake-2 models, we obtained the
13 corresponding forcing time series by averaging these observed quantities over the entire Lake
14 Erie. We adjusted the long-term mean of the observed $T_{a,u}(t)$ to best match the observed
15 evolution of the Great Lakes, and, in particular, the abrupt warming that took place between
16 1996/97 and 1997/98. *This adjustment was performed independently for each lake model and*
17 *each parameter set used in these models* (see **Table 2** below). The $T_{wind}(t)$ time series for the
18 two lake models was obtained by averaging the observed 925-mb temperature data over the
19 corresponding green boxes in Fig. 1 (bottom right). For each region, we also adjusted the long-
20 term mean of $T_{wind}(t)$ to match the long-term mean of the boundary-layer temperatures over the
21 corresponding lake.

22 We considered four different sets of adjustable parameters R and α (Table 2). The value of R
23 was either set to zero (no land) or unity (area of the land is equal to the lake area), and we used

1 three different values for the upwind advection efficiency α . Overall, the parameter set 1 is the
2 one in which the environment external to the lakes affects the lake evolution the most, whereas
3 the external effects become progressively weaker for the parameter sets 2, 3 and 4.

4 The effect of upwind advection efficiency parameter α on the lake response to external
5 warming is illustrated in **Table 3**, which shows the change in the summertime maximum surface
6 water temperature of Lake 1A subjected to the 4°C increase in the annual-mean $T_{a,u}(t)$ free-
7 atmosphere forcing, all other external atmospheric parameters being fixed at their (seasonally
8 evolving) 1998 conditions. When the upwind advection is too strong, the lake becomes
9 unrealistically insensitive to the increase of $T_{a,u}$. For example, with $\alpha = 1.0$, the summertime
10 maximum surface temperature of the lake only changes by 0.57°C. On the other hand, values of
11 α between 0.05 and 0.2 (Table 2) result in better matches between the observed and simulated
12 lake warming.

13 Finally, for each combination of models and parameters listed in Table 2, we also considered
14 two sets of simulations, in which the ice albedo was either set to its default value of 0.45
15 (comparable to the average ice albedo of 0.52 over the Great Lakes; see Zhong et al. 2016), or to
16 the open-water value of 0.05. In the latter case, the ice–albedo effect was thus artificially
17 suppressed. The comparisons between these two sets of experiments thus elucidate the role of the
18 ice–albedo feedback in the lake-system dynamics and its response to changes in the external
19 forcing.

20 *c. Observational data sets*

21 We compared our model simulations with the observational data from two sources: the
22 buoy data from the National Oceanic and Atmospheric Administration’s (NOAA) National Data

1 Buoy Center (NDBC: <http://www.ndbc.noaa.gov>), and the satellite data from the Great Lakes
2 Surface Environmental Analysis (GLSEA: <https://coastwatch.glerl.noaa.gov/glsea/>) by the
3 NOAA's Great Lakes Environmental Research Laboratory (GLERL).

4

5 **3. Results**

6 *a. Simulations of deep vs. shallow lakes*

7 **Figure 2** compares the simulated surface temperature time series over the 200-m column of
8 the Lake 1 models (see Table 2) with the observations at the NDBC buoy station 45004 in the
9 eastern Lake Superior (the lake depth there is 237m). Analogous comparisons between the
10 surface temperature of the 15-m column of Lake 2 model and Lake Erie observations (NDBC
11 buoy station 45005, depth of 10 m) are presented in **Fig. 3**. The deep-lake simulations (Fig. 2)
12 reproduce fairly well the seasonal cycles of lake-surface temperature for individual years, as well
13 as long-term changes in the shape and magnitude of these seasonal cycles. In particular, before
14 1998, Lake Superior preferentially exhibited the seasonal cycle characterized by an extensive
15 wintertime ice cover and cool summertime temperatures, whereas after 1998 a warmer, largely
16 ice-free seasonal cycle regime clearly became dominant. The simulations using different
17 parameter sets display instructive differences in capturing this regime change, which we will
18 analyze in greater depth and detail throughout the remainder of this paper.

19 In general, the deep-lake simulations with the ice albedo set to the default value of 0.45
20 performed much better in representing the cold years than the simulations in which the ice
21 albedo was set to the open-water value of 0.05, indicating an important role of the ice–albedo
22 feedback in controlling the observed regional climate change over deep lakes. For example,

1 extensive ice coverage during winter of 1993/94 resulted in cold lake-surface temperatures in the
2 following summer, which were much better simulated by the model versions that included the
3 ice–albedo effect vs. those in which ice–albedo effect was suppressed: compare the solid and
4 dotted black curves for summer 1994 in Figs. 2a,b. In contrast to the Lake Superior case, long-
5 term changes in the observed and simulated seasonal cycles of shallow Lake Erie (Fig. 3) are less
6 pronounced, and the model versions with the ice albedo of 0.05 in fact performed better than
7 those with the default ice-albedo value in capturing the late spring–early summer upswing of the
8 lake-surface temperature.

9 The discrepancies between the skill of our deep-lake and shallow-lake models in capturing the
10 observed seasonal cycles can also be visualized by displaying the observed and simulated long-
11 term mean seasonal cycles of Lake Superior and Lake Erie (**Fig. 4**). For all deep-lake
12 simulations with the ice albedo of 0.45, the simulated seasonal cycles are within 2°C of the
13 observed cycle throughout the year (Fig. 4a), whereas the simulations with the albedo value of
14 0.05 tend to exhibit a more substantial warm bias in summer and fall (Fig. 4b). For the shallow
15 lakes, the situation is reversed in the sense that the simulations without ice–albedo effect (Fig.
16 4d) match the observed seasonal cycles better than the simulations that include ice–albedo effect
17 (Fig. 4c). In the latter case, the simulated late-spring–mid-summer lake-surface temperatures
18 exhibit a substantial cold bias, especially in the simulations using parameter sets 1 and 2 from
19 Table 2.

20 This behavior can be traced to that of the simulated ice cover, with our models simulating ice
21 duration over deep-lake regions reasonably well (**Fig. 5**). Generally, if the observed surface
22 water temperature at buoy station 45004 dips below 1°C, it is a good indication that regions in
23 the vicinity of this station become ice-covered. Such periods occurred, for example, in the

1 winters of 1995/96, 1996/97, and 2002/03, and three out of our four configurations of our deep-
2 lake model capture this behavior (Figs. 5b–d). By contrast, our shallow-lake models with ice–
3 albedo feedback tend to overestimate the observed ice-season duration (**Fig. 6**, solid black),
4 which translates into a cold bias of the simulated seasonal cycles through the mid-summer, as per
5 Fig. 4c. In the absence of the ice–albedo feedback, the simulated ice-cover duration over shallow
6 lakes happens to match observations better (Fig. 6, dash-dotted curves), and so do the lake-
7 surface temperatures throughout the year (Fig. 4d).

8 Another, a somewhat more subtle but important issue evident from a careful analysis of Fig. 6
9 relates to the overestimation of the ice-duration *variance* by our shallow-lake models using the
10 better parameter sets 3 and 4 (“better” in terms of the match of their simulated Lake Erie
11 behavior with observations, per Figs. 3, 4 and 6). For example, in the simulation utilizing set 3
12 (Fig. 6b), the model produces no ice in 1998–2002, whereas observations indicate non-zero ice
13 coverage there. However, when the ice does appear in the simulations (in years 1996, 1997,
14 2003), the model generally overestimates the observed duration of the ice season. This
15 overestimation of the ice-season duration variance by our shallow-lake models indicates that
16 these models overestimate the strength of the ice–albedo feedback. The deep-lake simulations
17 perform much better in this regard, but might not be entirely free of this problem either, as they
18 also tend to overestimate somewhat the duration of the ice season in cold years (see Fig. 5).

19 In further presentation below, we will focus on analyzing the roots of the dramatic decadal
20 warming observed over deep regions of Lake Superior; the results of the present section argue
21 that our Lake 1 models are adequate for this purpose.

22

23

1 *b. Lake Superior regime shift of 1997/98*

2 Van Cleave et al. (2014) demonstrated that the recent persistent shift of Lake Superior to
3 warmer seasonal cycles with substantially reduced ice cover had a jump-like character (see Fig.
4 2); recognizing that, Zhong et al. (2016) concentrated on the 1997/98 transition to study the
5 dynamics of this shift using regional coupled lake–ice–atmosphere model with the state-of-the-
6 art atmospheric formulation. Their simulations reproduced a major fraction (68%) of the
7 observed July–August–September (JAS) mean temperature jump between the 1996/97 and
8 1997/98 seasonal cycles of Lake Superior, but only rationalized about 40% of the observed long-
9 term JAS surface-temperature trend over this lake (**Table 4**). The 1997/98 warming in their
10 model was due to the lake response to variable atmospheric forcing amplified by lake dynamics;
11 however, the simulated Lake Superior temperatures before this regime shift were on average
12 warmer than the observed temperatures, thus leading to the simulated decadal warming trend that
13 was much weaker than the observed trend. These results were also insensitive to the ice-albedo
14 value in their model, which prompted the authors to conclude that the lake-ice–albedo feedback
15 played little role in the observed warming of the Great Lakes.

16 By contrast, our Lake 1 model that best fits observations — the one using parameter set 3
17 from Table 2 and the ice-albedo value of 0.45 — is able to reproduce not only much (82%) of the
18 1997/98 JAS temperature jump over Lake Superior (**Fig. 7a**), but also about 94% of the observed
19 summertime decadal warming (Fig. 7c); see, once again, Table 4. Furthermore, the same model
20 configuration, but with the ice–albedo effect artificially suppressed (Figs. 7b,d), is only able to
21 capture less than 60% of both the observed 1997/98 temperature increase and of the long-term
22 decadal trend (Table 4). Hence, in the absence of ice–albedo feedback, our model, while
23 underperforming Zhong et al.’s (2016) model in capturing the magnitude of the 1997/98 Lake

1 Superior warming episode, shows a weaker-than-observed long-term warming consistent with
2 that in Zhong et al. (2016); the latter match is also consistent with the implied unimportance of
3 the ice–albedo feedback in the Zhong et al. (2016) model. The decadal warming in our model
4 with the suppressed ice–albedo feedback is weaker than the observed decadal warming due to
5 much the same reason as that simulated by the Zhong et al. (2016) model; namely, due to the
6 model’s inability to simulate well cold Lake Superior conditions in years 1982–1997 preceding
7 the transition to the warmer regime (see, for example, Fig. 2c).

8 We argue here, following Sugiyama et al. (2017) that decadal persistence of the cold Lake
9 Superior state during 1982–1997 is a manifestation of nonlinear lake dynamics rooted in the ice–
10 albedo feedback. In particular, under identical (seasonally varying) external forcing, our lake
11 models with an active ice–albedo feedback can exhibit multiple stable equilibrium seasonal
12 cycles, which differ by their respective wintertime ice coverage and maximum summertime
13 temperatures. The existence and basins of attraction of each regime depend on the external large-
14 scale forcing, with colder or warmer regimes being preferred in colder or warmer large-scale
15 environments, respectively. We thus propose that the observed decadal persistence of the Lake
16 Superior cold state prior to the 1997/98 transition, and the ensuing persistent warm state, reflect a
17 forced shift in preference from a colder to a warmer trait of multiple nonlinear regimes of the
18 type our model exhibits. We will present some concrete evidence for this regime dynamics
19 below in section 3c.

20 The relative role of the nonlinear dynamics discussed above — and the degree of
21 correspondence between observed and simulated regional climate change over Lake Superior —
22 decreases in the simulations which use parameter sets reflecting a progressively larger influence
23 of upwind atmospheric or adjacent land-surface conditions (Table 2) on lake’s response (**Fig. 8**).

1 As expected, the surrounding environment acts as a damping to reduce the effect of positive lake
2 feedbacks on the behavior of the coupled system, thus resulting in a weaker-than-observed
3 warming in the corresponding model simulations.

4 *c. Role of nonlinear regional climate regimes in Lake Superior warming*

5 While multiple nonlinear regimes in our lake models can occur under identical seasonally
6 varying forcing (Sugiyama et al. 2017), the actual climate forcing that may have induced the
7 1997/98 climate transition of Lake Superior wasn't constant, but exhibited a warming signal in
8 the atmospheric temperature over Great Lakes associated with the strong El Niño event (Van
9 Cleave et al. 2014; Gronewald et al. 2015; Zhong et al 2016). Furthermore, there is also evidence
10 for a larger-scale climatic shift that occurred at around the same time (Mukhin et al. 2015),
11 giving rise to two different — colder and warmer — decadal atmospheric environments over
12 Great Lakes before and after 1997/98. This shift can arguably be associated with the Pacific
13 Decadal Oscillation (Mantua et al. 1997) and can partially explain the decadal persistence of
14 warmer Great Lakes conditions in the post-1997 period (Zhong et al. 2016). In this section, we
15 examine relative roles of the Lake Superior forced response vs. its internal regime dynamics in
16 the 1997/98 transition to a warmer regional climate. To do so, we performed and analyzed initial
17 condition replacement experiments previously used by Zhong et al. (2016) to study the lakes'
18 dynamical memory in their model.

19 In these experiments (**Fig. 9**), we first ran lake simulations under the 1996/97 external forcing,
20 but using the lake/lake-ice initial conditions set to the corresponding conditions from year
21 1997/98 of the coupled model control simulation. For example, in the 1996/97 December
22 replacement experiment, we used the lake/ice conditions from December 1, 1997 to initialize the
23 model on December 1, 1996; we repeated these replacement experiments for a range of initial

1 conditions starting on the first of each month from January through July (Fig. 9a). Similarly, we
2 ran analogous replacement experiments in which the 1996/97 initial conditions were used in
3 conjunction with the 1997/98 history of external forcing (Fig. 9b). The model results shown in
4 Fig. 9 utilized parameter set 1 from Table 2, representing the situation with the strong effect of
5 upwind air advection on the lake's climate response; this set has the most pronounced contrast
6 between the simulations with and without active ice–albedo feedback.

7 Nonlinear regime dynamics of the simulated 1997/98 warming is reflected in our model's
8 trajectory being attracted to the warm climate regime when the cold lake/ice state of March 1,
9 1997 is reset to the warmer, ice-free state of March 1, 1998 (Fig. 9a, green curve); this also
10 happens in all other spring/summer 1997 replacement experiments in which the initial conditions
11 are substituted by those from year 1998. In all these cases, the coupled model still recovers a
12 major fraction of the 1997/98 warming despite being forced by colder 1996/97 external forcing.
13 On the other hand, for initial condition replacement on dates before March 1, 1997, the model's
14 climate quickly goes back to the current cold regime, and essentially simulates a trajectory (Fig.
15 9a, purple and blue curves) very similar to that of the unperturbed control experiment (Fig. 9a,
16 black curve). There is thus a discontinuity in the lake's summertime response to perturbed initial
17 conditions in the warm-perturbation experiments of year 1997 due to the presence of ice-albedo
18 induced multiple regional climate regimes of the coupled lake–ice–atmosphere system.

19 By contrast, when the lake's warm states of 1998 are replaced with the corresponding cold
20 states of 1997 (Fig. 9b), the model still exhibits, in each case, a substantial wintertime ice cover,
21 but summertime temperatures that are much warmer than their 1997 analogue due to the 1998's
22 external forcing being on average warmer than that of 1997. This relative warming is much aided
23 by the ice–albedo feedback, by which shorter ice season under warmer forcing results in

1 substantial enhancement of the net shortwave radiation absorbed by the lake in mid-spring. The
2 results of these experiments show a more continuous behavior with respect to the initial
3 condition replacement date, reflecting the (quasi-linear) dynamical memory of the lake within
4 the single (cold) regime.

5 The asymmetry between the 1997 and 1998 initial condition replacement experiments, which
6 is, once again, an indication of nonlinear regime dynamics operating in our coupled model, is
7 well seen in the lake-memory diagrams of **Fig. 10a**, which show the fraction of the maximum
8 summertime difference between the 1997 and 1998 seasonal cycles of the control run realized in
9 the initial condition replacement experiments. The 1997 replacement results exhibit a jump in the
10 fraction of the explained warming on and after March 1, due to the occurrence of persistent
11 regime transition there, whereas the 1998 replacement results show more gradual changes as the
12 initial condition replacement date progresses forward toward summer. No such asymmetry
13 occurs in the coupled model version in which the ice–albedo feedback is artificially suppressed
14 and the multiple nonlinear climate regimes do not exist (Fig. 10b). The only discontinuity in the
15 latter experiments is associated with the fact that the atmospheric forcing conditions in June of
16 1997 were in fact warmer than June 1998 conditions (despite 1998 was warmer than 1997 for all
17 other months), thus resulting in the anomalously high bar corresponding to the June replacement
18 experiment.

19 These results are also reproduced in the Lake 1 model with parameter set 3 of Table 2, which
20 corresponds to a smaller influence of the surrounding environment on the lake behavior; this
21 parameter set is the one that achieves the best correspondence between the simulated and
22 observed long-term warming of Lake Superior in our model (Fig. 8c). In this case, the lake
23 initialized in as early as February by the warmer 1998 state is able to maintain its warm regime

1 and stay ice-free under the colder 1997 external forcing (**Fig. 11**). Even earlier — Dec. 1996 or
2 Jan. 1997 — replacement ends up in the cold regime state, thus rationalizing the jump in the
3 fraction of the explained warming between January and February replacement experiments, as
4 well as the asymmetry between the 1997 (blue bars) and 1998 (yellow bars) February–May
5 replacement experiments (that is, a larger fraction of the 97/98 temperature difference explained
6 in the 1997 replacement experiments relative to the 1998 replacement experiments). Note that
7 despite the apparent differences between our model and that of Zhong et al. (2016), the diagram
8 in Fig. 11 is quantitatively very similar to the analogous diagram in Zhong et al. (2016),
9 indicating that both of these models provide plausible scenarios of the regional climate change
10 associated with lake dynamics. The similarity of our results to those of a much more
11 sophisticated regional model of Zhong et al. also indicates that the parameters in our
12 representation of the upwind atmospheric influence (1) are reasonable.

13 Zhong et al. (2016) argued that the ice–albedo feedback plays little role in the 1997/98
14 warming of Lake Superior, partly because the net fraction of the 1997/98 warming computed by
15 averaging the results of 1997 and 1998 March replacement experiments in their model was large
16 (56%), the argument here being that the lake ‘remembers’ March initial conditions well into
17 summer despite the potential of the lake-ice–albedo feedback to destroy this memory is strongest
18 in Spring. However, in our model, where the ice–albedo feedback is clearly important for the
19 correct simulation of the Lake Superior’s observed warming, this net fraction is 52% (Fig. 11),
20 which is very close to the value reported by Zhong et al. (2016). In our present interpretation, the
21 lake-ice–albedo feedback is instrumental in regulating the 1997/98 warming of Lake Superior in
22 our coupled model simulations, via its nonlinear control over the preference for the warmer or
23 colder regime under warmer or colder external forcing, thus explaining the decadal persistence of

1 the Lake Superior anomalous conditions on either side of the 1997/98 transition (Fig. 8c) that
2 Zhong et al.'s (2016) model couldn't quite capture.

3 *d. Onset of summertime stratification*

4 Zhong et al. (2016) argued that despite the observed (negative) correlation between the
5 wintertime lake-ice coverage and summertime surface temperature over Great Lakes (Hanrahan
6 et al. 2010), the two are not causally connected via the ice–albedo feedback (as suggested by
7 Austin and Colman 2007), but rather reflect the lake's response to a common external factor
8 associated with the severity of wintertime atmospheric conditions. The lake-ice coverage is
9 affected by these conditions directly, while their effect on lake-surface temperature in the
10 following summer occurs through the associated adjustment of the onset of summertime mixed
11 layer. Indeed, in both Zhong et al.'s (2016) model and our present model, correct simulation of
12 the date on which a deep lake stratifies in spring or summer (that is, the date on which its surface
13 water temperature reaches 3.98°C for the first time after winter) is essential for reproducing the
14 observed warming rates of deep lakes. Before that date within a given year, the lake's surface
15 temperature increases very slowly under seasonal external warming, since the heat is being
16 spread out most of the water column. As stratification sets in, the seasonal heating gets trapped
17 within a shallow mixed layer, and surface warming rates increase rapidly (**Fig. 12**). Therefore,
18 the stratification onset date largely controls the maximum temperature the deep lakes can achieve
19 in summer, with later dates leading to cold summers and vice versa.

20 Here we examine the observed and simulated seasonal cycles over the 1988–2007 period to
21 assess, indirectly, the importance of the ice–albedo feedback in the Lake Superior warming
22 during this period. The observed seasonal cycles at the eastern buoy station 45004 exhibit large
23 spread of the summer stratification start dates on the order of two months (Fig. 12a), which

1 reflect the differences between lake's seasonal cycles in the (late onset, colder) first and (early
2 onset, warmer) second part of the period considered. Our model simulations with parameter set 1
3 (Figs. 12c,d) — strongly controlled by ambient external conditions, — as well as parameter set 3
4 without the ice–albedo feedback (not shown) all underestimate the observed spread of the
5 stratification onset dates by a factor of two or so. The same discrepancy is a feature of the Zhong
6 et al.'s (2016) simulations, in which the spread of the deep Lake Superior summertime
7 stratification onset dates over the past decades is only around one month. By contrast, our best
8 simulation with parameter set 3 and the ice albedo value of 0.45 matches the observations much
9 better, with the simulated spread of stratification start dates of around 50 days (Fig. 12b).

10 The latter property provides further support for the important role of the ice–albedo feedback
11 in controlling the magnitude of the observed decadal warming of deep Great Lakes through
12 regulating the late spring/early summer lake-surface temperature. These temperatures in turn
13 control the start date of summertime thermal stratification, as indicated by the linear relationship
14 between the two (**Fig. 13a**). The latter relationship is, once again, fairly well reproduced by our
15 best model (parameter set 3) with the ice–albedo feedback, both in terms of the slope and in
16 terms of the spread of stratification-onset dates and lake-surface temperatures (Fig. 13b). The
17 models with the suppressed ice–albedo effect, on the other hand, are unable to simulate very late
18 stratification onset dates in the pre-1998 decade, and thus underestimate the magnitude of
19 decadal-scale deep-lake warming initiated in year 1998 (Fig. 13c), which is similar to the results
20 of Zhong et al. (2016). Perhaps not surprisingly, the same arguments apply to our models' ability
21 to simulate realistic variations of deep-lake surface temperatures in late summer (Figs. 13d–f),
22 since the late-summer warming is intimately linked to the length of the stratified season. In
23 particular, our models that include albedo feedback capture well (Fig. 13e) — and those without

1 the ice–albedo feedback (Figs. 13f) underestimate — the observed variance of the August-mean
2 temperature (Fig. 13e). The lack of variance in late-summer lake-surface temperatures is, once
3 again, also a feature of the simulations in Zhong et al. (2016). This suggests that, in these
4 simulations, some counteracting mechanism, such as the ice insulation effect, cancels the effects
5 of the ice–albedo feedback in spring, which ultimately introduces a warm bias in the simulated
6 cold-year springtime temperatures, earlier-than-observed stratification onset dates, and late-
7 summer temperatures that are closer to those during the warm years than the observations
8 indicate.

9 *e. Correlation between lake bathymetry and warming rates*

10 The Great Lakes exhibit clear positive correlation between lake depth and surface warming
11 trends, by which deeper lake regions tend to warm faster than shallow regions (Zhong et al.
12 2016; Sugiyama et al. 2017). In particular, the deepest areas of Lake Superior warmed faster than
13 the rest of the lake, both in terms of their 1997/98 surface-temperature jump, and in terms of the
14 long-term 1988–2007 trend. Yet, many such deep areas remained largely ice-free in both 1997
15 and 1998, while their net longer-term 1988–2007 lake-ice decrease was slight compared to that
16 over other, shallower areas. Zhong et al. (2016) argued that this property provides further
17 evidence for a limited role of ice–albedo feedback in the observed warming of the Great Lakes.

18 To further explore this issue, we studied long-term changes in the ice coverage (**Table 5**) and
19 surface temperature (**Fig. 14**) over different columns of our Lake-1 models, using parameter sets
20 3 and 4 of Table 2 and ice-albedo values of 0.45 (full model) and 0.05 (ice–albedo feedback
21 artificially suppressed). Curiously, in both models with suppressed ice–albedo feedback, the
22 deepest column exhibits the fastest warming rate compared to other columns — albeit only
23 about half as large as the observed warming rate (Figs. 14b,d) — but, at the same time, the

1 *slowest* rates of long-term lake-ice decrease (Table 5b,d). From the models with ice–albedo
2 feedback included, the model using our best parameter set 3 does also reproduce the observed
3 correlation between the warming rates and lake depths (Fig. 14a), whereas in the alternative
4 model with parameter set 4, the deepest column exhibits, in fact, a slightly slower surface
5 warming rate compared to those over other columns (Fig. 14c). This behavior is not linearly
6 connected with relative rates of the lake-ice decrease over the different columns of these models.
7 In the model with parameter set 3, the deepest column exhibits the lake-ice decrease of about
8 80% that over the intermediate column, but exceeding much that of the shallowest column
9 (Table 5a); thus, the combination of lake/ice dynamics leads to the fastest warming rates over the
10 deepest column there. The model that uses parameter 4, on the other hand, is characterized by the
11 deepest-column lake-ice decrease which is much slower than those over the intermediate or
12 shallow columns (Table 5c); however, the summertime surface warming rates are fairly uniform
13 throughout the entire lake in this case (Fig. 14c).

14 A take-away message here is that the relationship between the lake depth, long-term changes
15 in lake-ice coverage and lake-surface temperature is a complex function of the ice–albedo
16 feedback, as well as other feedbacks operating in the coupled lake–ice–atmosphere system. This
17 relationship may be further contaminated by the sampling variations in external forcing and the
18 associated lake response. Our best model provides a proof-of-concept example in which the
19 deep-lake region loses ice slower than the intermediate-depth region, but still exhibits the fastest
20 warming. Note, however, that our model is idealized, and inclusion of other physical processes
21 — most notably, interactive lake circulation — may modify the interplay between the forced
22 response and internal lake dynamics and lead to a better simulation of the observed lake warming.

23

1 **4. Summary and discussion**

2 We used an idealized coupled lake–ice–atmosphere model of Sugiyama et al. (2017) to
3 examine the dynamics of the recent accelerated warming of the Great Lakes. Under identical
4 seasonally varying forcing, this model can exhibit multiple stable seasonal cycles, or regimes.
5 Colder regimes are characterized by massive wintertime ice cover and cool lake-surface
6 temperatures in summer, while warmer regimes show little-to-no-ice and higher summertime
7 temperatures. The regimes’ existence is rooted in the ice–albedo feedback, as the model in which
8 this feedback is artificially suppressed exhibits no regime behavior (Sugiyama et al. 2017). The
9 main focus of this research was to study the response of our regime-permitting coupled model to
10 the external large-scale warming over the 1988–2007 period.

11 The lake component of the coupled model consisted of three lake columns representing deep,
12 intermediate-depth and shallow lake regions. We used several model configurations that
13 mimicked the bathymetry and external forcing of the Lake Superior and Lake Erie, and explored
14 sensitivity of the model’s response to adjustable parameters, including, most importantly, the
15 lake-ice albedo. Our best Lake Superior model with an active ice–albedo feedback is able to
16 capture both the lake’s 1997/98 transition to warmer regional climate conditions, as well as the
17 decadal persistence of the warm and cold state on either side of this transition, leading to the
18 correct simulation of the observed decadal warming of Lake Superior. By contrast, the same
19 model configuration, but with ice–albedo feedback artificially suppressed, can only capture
20 about 60% of the observed warming (by failing to simulate cold enough pre-1998 conditions),
21 thus assigning the remaining 40% of the warming to the action of the ice–albedo feedback. Our
22 models of the shallow Lake Erie perform worse than those of deep Lake Superior, and generally
23 tend to overestimate ice-season duration, leading to cold surface-temperature bias in spring and

1 early summer; this bias is alleviated in the models with the ice albedo set to the open-water value.
2 However, in either configuration, the acceleration of the estimated mid-summer/early-fall Lake
3 Erie warming in response to large-scale climatic forcing is less pronounced than that over Lake
4 Superior, as observed.

5 The most striking implication of our experiments is in re-establishing the importance of the
6 ice–albedo feedback in regulating the magnitude of the accelerated lake warming (compare with
7 the pioneering work of Austin and Colman 2007). The control exerted by the ice–albedo
8 feedback here is, however, fundamentally nonlinear, arising through its key role in the simulated
9 regime dynamics. In particular, under colder 1988–1997 external conditions, the occurrence of
10 the cold regime in our model is preferred over that of the warm regime, whereas the situation is
11 reversed during warmer 1998–2007 conditions, under which the warm regime becomes dominant.
12 The direct forced warming of the lake is thus amplified by internal nonlinear regime dynamics,
13 thereby explaining the enhanced, more realistic, magnitude of the warming simulated by our full
14 model relative to the one in which the ice–albedo feedback was artificially suppressed.

15 The regime nonlinearity is also behind the discontinuity of the lake’s memory found in the
16 experiments in which the lake model was initialized by warmer states of year 1998, but forced by
17 colder external conditions corresponding to year 1997. In cases when such initial condition
18 replacement was performed early in the year, the external forcing was able to shift the model
19 back to its cold regime, and only a small fraction of the full 1997/98 summertime temperature
20 difference was eventually realized. However, for late winter/early spring replacements, the
21 coupled system got stuck in the warm regime, suddenly resulting in a major fraction of the
22 explained summertime warming. Naturally, no such discontinuity was found in the replacement
23 experiments with the model in which the ice–albedo feedback was artificially suppressed. Note

1 that, in our late winter/early spring replacement experiments, the fact that the largely *ice-free*
2 1998 initial conditions still account for a major portion of the full summertime warming despite
3 colder external forcing does not indicate the unimportance of lake-ice–albedo feedback in this
4 warming, since the ice–albedo feedback is instrumental in the existence of the warm and cold
5 regimes in our model in the first place (compare with Zhong et al. 2016).

6 Zhong et al. (2016) emphasized the response of the onset date of the summertime
7 stratification to the long-term changes in the wintertime external forcing as the major cause of
8 the Lake Superior accelerated warming in their model. This is also the case in our simulations, as
9 the date of the summertime mixed layer formation is one of the major differences between our
10 simulated cold and warm regimes (note, however, that the albedo–driven regime dynamics is still
11 the primary cause of these differences). In fact, only our best regime-permitting simulation with
12 an active ice–albedo feedback is able to capture the observed spread of the stratification onset
13 dates for deep Lake Superior, whereas the same model with the ice–albedo effect suppressed, as
14 well as Zhong et al.’s model, underestimate this spread by factor of two or so due to failing to
15 simulate extremely late onset dates in the 1988–1997 cold period.

16 When the Lake Superior climate change is interpreted as the shift in the preferential
17 occurrence of its cold and warm regimes, the distinction between warm- and cold-regime
18 seasonal cycles helps also explain the observed long-term correlation between lake’s wintertime
19 ice cover and lake-surface temperature in the following summer (Hanrahan et al. 2010).
20 Furthermore, since the differences between the warm and cold regimes simulated by our best
21 model become progressively more dramatic in deeper lake columns, the regime occurrence shift
22 matches the observed correlation between local warming rate and local lake depth within
23 individual Great Lakes (Zhong et al. 2016; Sugiyama et al. 2017). Note that in our best

1 simulation, the warming over the deepest lake column is the strongest despite its ice-loss rate is
2 slower than that over the intermediate-depth column, which demonstrates that the regime-
3 dependent warming is a complex function of internal lake dynamics (including ice–albedo and
4 other feedbacks), as well as externally forced response. Incidentally, this situation is also a
5 feature of the observed warming of Lake Superior, where the strongest warming rates often
6 occurred in the regions of moderate or little ice loss; our results indicate that this does not mean
7 that ice–albedo feedback is necessarily unimportant in the accelerated lake warming, as Zhong et
8 al. (2016) argue.

9 Zhong et al. (2016) regional coupled model simulated much of the observed 1997/98 climate
10 shift of Lake Superior, but showed only a modest skill in capturing the magnitude of decadal-
11 scale climate change over that lake, matching roughly the performance of our lake model with
12 suppressed ice–albedo effect and, hence, suppressed regime dynamics. This is consistent with the
13 implied limited role of the ice–albedo feedback in Zhong et al. (2016) model, as their simulations
14 with or without the inclusion of this feedback essentially produced identical results. We
15 speculate here that the differences between Zhong et al. model and the present model stem
16 primarily from the apparent lack of regime dynamics in the former, most probably due to the
17 differences in the lake-ice model formulation and the lake model’s convective mixing scheme,
18 leading to a decreased role of the ice–albedo feedback in Zhong et al. model and the resulting
19 excessive warmth of their cold-year simulated climates. Alternatively, of course, regime
20 dynamics detected in our simulations may be an artifact of extremely low horizontal model
21 resolution or overly idealized atmospheric formulation. Finally, neither our model nor that of
22 Zhong et al. (2016) included interactive lake circulation (see, for example, Beletsky et al. 1999;

1 Beletsky and Schwab 2001), which could potentially affect both the model's internal dynamics
2 and its response to the external forcing. All of these issues are to be addressed in future research.

3 While our coupled model is able to reproduce many intricate characteristics of the observed
4 accelerated warming of the Great Lakes, there are indications that these dynamics may not
5 universally apply to other mid-latitude lakes (Schneider et al. 2009; Schneider and Hook 2010;
6 O'Reilly et al. 2015), which does make the problem of lacustrine regional amplification of global
7 warming signal even more intriguing.

8

9 **Acknowledgements.** We thank Michael Notaro, Stephen Vavrus and Yafang Zhong for nu-
10 merous valuable discussions on the subject of this paper. This work was supported by the NSF
11 grant 1236620.

12

13

14

15

16

17

18

19

20

1 **References**

- 2 Ackerman, S., A. Heidinger, M. Foster and B. Maddux, 2013: Satellite regional cloud
3 climatology over the Great Lakes. *Remote Sensing*, **5**, 6223–6240.
- 4 Arvola, L., G. George, D. M. Livingston, M. Järvinen, T. Blenckner, M. T. Dokulil, E. Jennings,
5 C. N. Aonghusa, P. Noges, T. Noges and G. A. Weyhenmeyer, 2010: The impact of the
6 changing climate on the thermal characteristics of lakes. In: *The Impact of Climate Change on*
7 *European Lakes*, D. George, Ed. Aquatic Ecology Series, pp. 85–101, Springer, Netherlands.
- 8 Assel, R., K. Cronk and D. Norton, 2003: Recent trends in Laurentian Great Lakes ice cover.
9 *Clim. Change*, **57**, 185–204.
- 10 Austin J. and J. Allen, 2011: Sensitivity of summer Lake Superior thermal structure to
11 meteorological forcing. *Limnol. Oceanogr.*, **56**, 1141–1154.
- 12 Austin JA, Colman SM (2007) Lake Superior summer water temperatures are increasing more
13 rapidly than regional air temperatures: A positive ice-albedo feedback. *Geophys Res Lett* 34:
14 L06604
- 15 Beletsky, D., J. H. Saylor and D. J. Schwab, 1999: Mean circulation in the Great Lakes. *J. Great*
16 *Lakes Res.*, **25**, 78–93.
- 17 Beletsky, D. and D. J. Schwab, 2001: Modeling circulation and thermal structure in Lake
18 Michigan: Annual cycle and interannual variability. *J. Geophys. Res.*, **106**, 19745–19772.
- 19 Fink, G., M. Schmid, B. Wahl, T. Wolf and A. Wuest, 2014: Heat flux modifications related to
20 climate-induced warming of large European lakes. *Water Resour. Res.*, **50**, 2072–2085.
- 21 Foster, M. and A. Heidinger, 2013: PATMOS-x: Results from a diurnally corrected 30-yr
22 satellite cloud climatology. *J. Climate*, **26**, 414–425.
- 23 Gronewold, A. D., E. J. Anderson, B. Lofgren, P. D. Blanken, J. Wang, J. Smith, T. Hunter, G.
24 Lang, C. A. Stow, D. Beletsky and J. Bratton J, 2015: Impacts of extreme 2013–2014 winter

1 conditions on Lake Michigan's fall heat content, surface temperature, and evaporation.
2 *Geophys. Res. Lett.*, **42**, 3364–3370.

3 Hanrahan, J. L., S. Kravtsov and P. J. Roebber, 2010: Connecting past and present climate
4 variability to the water levels of Lake Michigan and Huron. *Geophys. Res. Lett.*, **37**, L01701.

5 Hostetler, S. and P. J. Bartlein, 1990: Simulation of lake evaporation with application to
6 modeling lake-level variations at Harney-Malheur Lake, Oregon. *Water Resour. Res.*, **26**,
7 2603–2612.

8 Karlsson K.-G., A. Riihela, R. Muller, J. F. Meirink, J. Sedlar, M. Stengel, M. Lockhoff, J.
9 Trentmann, F. Kaspar, R. Hollmann and E. Wolters E, 2013: CLARA-A1: the CM SAF
10 cloud, albedo and radiation dataset from 28 yr of global AVHRR data. *Atmos. Chem. Phys.*
11 *Discuss.*, **13**, 935–982, doi:10.5194/acpd-13-935-2013.

12 Magnuson, J. J., 2000: Historical trends in lake and river ice cover in the Northern Hemisphere.
13 *Science*, **289**, 1743–1746, doi:10.1126/science.289.5485.1743.

14 Mantua, N. J., Y. Zhang, J. M. Wallace, R. C. Francis, 1997: A Pacific interdecadal climate
15 oscillation with impacts on salmon production. *Bull. Amer. Meteor. Soc.*, **78**, 1069–1079.

16 Mukhin, D., A. Gavrilov, A. Feigin, E. Loskutov and J. Kurths, 2015: Principal nonlinear
17 dynamical modes of climate variability. *Nature Sci. Rep.*, **5**, 15510, doi:10.1038/srep15510.

18 O'Reilly, C. M., S. Sharma, D. K. Gray, S. E. Hampton, et al., 2015: Rapid and highly variable
19 warming of lake surface waters around the globe. *Geophys. Res. Lett.*, **42**, 10773–10781,
20 doi:10.1002/2015GL066235

21 Piccolroaz, S., M. Toffolon and B. Majone, 2015: The role of stratification on lakes' thermal
22 response: The case of Lake Superior. *Water Resour. Res.*, **51**, 7878–7894, doi:10.1002/
23 2014WR016555.

1 Schneider P. and S. J. Hook, 2010: Space observations of inland water bodies show rapid
2 surface warming since 1985. *Geophys. Res. Lett.*, **37**, L22405.

3 Schneider, P., S. J. Hook, R. G. Radocinski, G. K. Corlett, G. C. Hulley, S. G. Schladow and T.
4 E. Steissberg, 2009: Satellite observations indicate rapid warming trend for lakes in California
5 and Nevada. *Geophys. Res. Lett.*, **36**, L22402, doi:10.1029/2009GL040846.

6 Semtner, A. J., 1976: A model for the thermodynamic growth of sea ice in numerical
7 investigations of climate. *J. Phys. Oceanogr.*, **6**, 379–389.

8 Sugiyama, N., S. Kravtsov and P. J. Roebber, 2017: Multiple climate regimes in an idealized
9 lake-ice-atmosphere model. *Climate Dyn.*, sub judice. Preprint available from
10 <https://people.uwm.edu/kravtsov/publications/>.

11 Van Cleave, K., J. D. Lenters, J. Wang and E. M. Verhamme, 2014: A regime shift in Lake
12 Superior ice cover, evaporation, and water temperature following the warm El Niño winter of
13 1997–1998. *Limnol. Oceanogr.*, **59**, 1889–1898, doi:10.4319/lo.2014.59.6.1889.

14 Vavrus, S., R. Wynne and J. Foley, 1996: Measuring the sensitivity of southern Wisconsin lake
15 ice to climate variations and lake depth using a numerical model. *Limnol. Oceanogr.*, **41**,
16 822–831.

17 Zhong, Y., M. Notaro and S. J. Vavrus, 2016: Recent accelerated warming of the Laurentian
18 Great Lakes: Physical drivers. *Limnol. Oceanogr.*, **61**, 1762–1786, doi: 10.1002/lno.10331.

19
20

1 **Table captions**

2 **Table 1:** Bathymetry of different lake models.

3 **Table 2:** Different combinations of adjustable parameters used in the paper.

4 **Table 3:** Increase ΔT ($^{\circ}\text{C}$) of the maximum summertime surface water temperature of Lake 1A
5 in response to the increase of the long-term mean free-atmosphere forcing temperature $T_{a,u}$ by
6 4°C , as a function of the upwind advection efficiency parameter α . The other forcing
7 parameters are fixed and correspond to the Lake Superior conditions in 1997.

8 **Table 4:** Percentages of the observed Lake Superior's July–August–September (JAS) mean
9 temperature difference simulated by Zhong et al.'s (2016) model and our best models with
10 and without the albedo feedback (that is, the models with the ice albedo values set to $a=0.45$
11 and $a=0.05$, respectively). Zhang et al.'s results are based on the temperature averages over
12 the entire lake, and use OISST2 product for observational estimates. The present results
13 compare the changes in surface temperature of our best model's deepest column (depth of
14 200m) with the surface-temperature record at the NDBC's buoy station 45004 (lake depth of
15 237m). *Note also that the long-term change in Zhong et al. (2016) is defined as the
16 difference between the average 1998–2012 and 1982–1997 JAS temperature, while in the
17 present paper it is defined as the JAS temperature difference between 1998–2007 and 1988–
18 1997 periods.

19 **Table 5:** Change in the wintertime ice coverage (days) from the 1998–1997 period to the 1998–
20 2007 period, for each column of Lake 1 models with four different combinations of albedo
21 parameter and adjustable parameters of Table 2. The same sets (a–d) are used in Fig. 14.

22

23

1 **Figure captions**

2 **Figure 1:** Coupled model geometry. Top: cross-section view; bottom left: plan view. Bottom
3 right: green shading denotes the regions used to compute upwind forcing temperature
4 $T_{wind}(t)$ [see (1) and section 2.2].

5 **Figure 2:** Observed and simulated time series of daily-mean surface water temperature ($^{\circ}\text{C}$) of
6 the eastern Lake Superior, with the simulated data coming from the Lake-1 models with (a)
7 Set 4, (b) Set 3, (c) Set 2, and (d) Set 1 parameter sets (Table 2). The purple dots show the
8 observed surface temperature time series based on the data from the NDBC surface buoy
9 station 45004 in the eastern Lake Superior (lake depth at this location is 237m). The red dots
10 are daily-mean surface water temperature at the same location based on the GLSEA data. The
11 simulated surface temperatures (black) are those over the 200-m column of each lake model
12 considered; solid curves correspond to model simulations with the lake-ice albedo set to 0.45,
13 and dash-dotted curves — to the simulations with the lake-ice albedo of 0.05 (dash-dotted
14 curves).

15 **Figure 3:** The same as in Fig. 2, but for the surface temperature observations of Lake Erie and
16 the simulations of Lake-2 model. The NDBC buoy data (purple dots) correspond to the Lake
17 Erie's buoy station 45005 (lake depth of 10m). The simulated time series shown are those for
18 surface temperatures over the 15-m column of Lake-2 model.

19 **Figure 4:** The observed and simulated 1995–2005 average seasonal cycles of surface water
20 temperature based on the data from Figs. 2 and 3. The observed cycles shown here were
21 computed using the GLSEA data. See panel captions and figure legend to identify the results
22 from different simulations listed in Table 2. Note that the results displayed here encompass
23 model simulations both with and without the ice–albedo feedback.

1 **Figure 5:** The close-up of the surface-temperature time series shown in Fig. 2 (Lake Superior)
2 restricted to the 1996–2004 period and to the 0–5°C range of lake-surface temperatures to
3 emphasize the cold-season temperature variability.

4 **Figure 6:** The same as in Fig. 5, but for the close-up view of the Lake Erie time series of Fig. 3.

5 **Figure 7:** The difference in the observed (red) and simulated (blue) seasonal cycle of the eastern
6 Lake Superior surface temperature between years 1998 and 1997 (top), as well as between the
7 10-yr-mean seasonal cycle based on 1998–2007 and 1988–1997 decades (bottom). We used
8 observations of surface temperature for NDBC buoy station 45004 in the eastern Lake
9 Superior (lake depth of 237m there), and simulations with Lake 1 model with parameter set 3
10 from see Table 2; shown here are simulated surface temperatures over the 200-m column of
11 this model. Left column of the figure: ice albedo was set to the default value of 0.45; left
12 column: ice albedo was set to the open-water value of 0.05.

13 **Figure 8:** The same as in Fig. 7, but for Lake 1 model simulations using parameter sets 1, 2 and
14 4 of Table 2 (see figure legend).

15 **Figure 9:** Initial condition replacement experiments for 1996/97–1997/98 warming simulated by
16 the Lake 1 model with parameter set 1 of Table 2 and the default ice-albedo value of 0.45. In
17 (a), solid black curve show the July 1, 1996–December 31, 1998 segment of the simulated
18 lake-average surface temperature time series. Black dotted curve, on the other hand, shows
19 the simulated surface temperature evolution shifted backwards by one year, thus
20 corresponding to the period from December 1, 1997 through December 31, 1998. Different
21 colored lines show the results of the simulations under the July 1, 1996–December 31, 1998
22 external forcing, in which the lake temperature and ice conditions were replaced, on a certain
23 date, by the conditions one year later; that is, the states reflected by the black solid curve were

1 replaced by the corresponding states on the black dotted curve. Replacement dates are given
2 in the panel legend. Panel (b) shows the results of the experiments analogous to those in (a),
3 except the roles of 1997 and 1998 were switched, that is, the 1996/97 initial conditions were
4 used in conjunction with the 1997/98 external forcing history. Vertical line in each panel
5 marks the location of the July 20 date.

6 **Figure 10:** Role of antecedent lake conditions in the simulated 1997/98 warming of Lake
7 Superior. Shown is the fraction of the simulated surface temperature difference between July
8 20, 1997 and July 20, 1998 (this difference peaks on July 20, hence the choice of the date)
9 realized in the initial condition replacement experiments of Fig. 9. For example, the blue bar
10 in panel (a) for month 3 measures the ratio of the difference between solid green and black
11 curves to the difference between dotted black and solid black curves in Fig. 9a, for July 20;
12 this ratio turns out to approximately equal 0.6: 60% of the full simulated warming thus
13 reflects lake's memory of the March initial conditions. The yellow bars in panel (a) show the
14 results based on the 1998 replacement experiments from Fig. 9b. Panel (b) shows analogous
15 results for the lake model in which the ice–albedo feedback was artificially suppressed. The
16 ratios shown in (b) still correspond to the July 20 date, as in (a).

17 **Figure 11:** The same as in Fig. 10a, but for the Lake 1 model with parameter set 3 of Table 2.

18 The date of maximum summertime temperature difference between 1997 and 1998 on which
19 the fractions of warming explained by the replacement experiments are recorded in these
20 simulations is August 8.

21 **Figure 12:** Spaghetti plots of observed and simulated May–October lake-surface temperature
22 time series for each year between 1988 and 2007. (a) Observed temperatures (NDBC's
23 eastern Lake Superior buoy 45004, depth of 237m); (b, c) Simulated 200-m column surface

1 temperatures for Lake 1 model with parameter sets 3 and 1, respectively (Table 2), and ice
2 albedo of 0.45; (d) The same as in (c), but for the model with the ice albedo set to 0.05.

3 **Figure 13:** Connection between the onset of summertime stratification and lake temperatures. (a)
4 Scatter plot of the daily-mean lake-surface temperatures at the NDBC buoy station 45004 in
5 the eastern Lake Superior on June 1 (before the onset of the stratification) versus the start
6 dates of summertime thermal stratification (that is, the date on which daily-mean lake-surface
7 temperature at this location warmed above 3.98°C for the first time after winter). The blue
8 dots correspond to years between 1988 and 1997, and the red dots correspond to years
9 between 1998 and 2007. (b) The same as in (a), but for the surface temperature of 200-m
10 column of Lake 1 model with parameter set 3 of Table 2 and the default ice-albedo value of
11 0.45; (c) the same as in (b), but for the Lake 1 model with parameter set 1 of Table 2 and the
12 ice-albedo value of 0.05. Panels (d–f) are analogous to (a–c), but document the connection
13 between the onset of stratification and August-mean lake surface temperature (that is, after the
14 onset of summertime stratification); note also that the axes here are flipped with respect to the
15 axes in panels (a–c).

16 **Figure 14:** The difference between the 10-yr-mean seasonal cycle of the eastern Lake Superior
17 surface temperature based on 1998–2007 and 1988–1997 decades, in observations and model
18 simulations. We used observations of surface temperature for NDBC buoy station 45004 in
19 the eastern Lake Superior (lake depth of 237m there) [red], and simulations of Lake 1 models
20 with Table 2 parameter sets 3 (top row) and 4 (bottom row). Shown are the simulated surface
21 temperatures over the 200-m (blue), 100-m (cyan) and 50-m (green) columns of these models.
22 Left column of the figure: ice albedo in the model was set to the default value of 0.45; right
23 column: ice albedo was set to the open-water value of 0.05.

1 **Table 1:** Bathymetry of different lake models.

Lake 1A	Depth	Relative area
Column 1	50m	10%
Column 2	100m	10%
Column 3	200m	80%
Lake 1B	Depth	Relative area
Column 1	50m	10%
Column 2	100m	80%
Column 3	200m	10%
Lake 2	Depth	Relative area
Column 1	15m	40%
Column 2	20m	50%
Column 3	40m	10%

2
3
4

Table 2: Different combinations of adjustable parameters used in the paper.

	R	α	Bathymetry
Set 1	1	0.2	Lakes 1A or 2
Set 2	0	0.2	Lakes 1A or 2
Set 3	0	0.1	Lakes 1A or 2
Set 4	0	0.05	Lakes 1B or 2

5
6

7 **Table 3:** Increase ΔT ($^{\circ}\text{C}$) of the maximum summertime surface water temperature of Lake 1A
8 in response to the increase of the long-term mean free-atmosphere forcing temperature $T_{a,u}$ by
9 4°C , as a function of the upwind advection efficiency parameter α . The other forcing parameters
10 are fixed and correspond to the Lake Superior conditions in 1998.

α	ΔT 11
0.05	2.7
0.1	2.6
0.2	1.8
0.4	1.0
1.0	0.57

12
13
14
15

1 **Table 4:** Percentages of the observed Lake Superior’s July–August–September (JAS) mean
 2 temperature difference simulated by Zhong et al.’s (2016) model and our best models with and
 3 without the albedo feedback (that is, the models with the ice albedo values set to $a=0.45$ and
 4 $a=0.05$, respectively). Zhang et al.’s results are based on the temperature averages over the entire
 5 lake, and use OISST2 product for observational estimates. The present results compare the
 6 changes in surface temperature of our best model’s deepest column (depth of 200m) with the
 7 surface-temperature record at the NDBC’s buoy station 45004 (lake depth of 237m). *Note also
 8 that the long-term change in Zhong et al. (2016) is defined as the difference between the average
 9 1998–2012 and 1982–1997 JAS temperature, while in the present paper it is defined as the JAS
 10 temperature difference between 1998–2007 and 1988–1997 periods.
 11

Results	1998–1997 JAS ΔT	Long-term* JAS ΔT
Zhong et al. (2016)	68%	42%
This paper ($a=0.45$)	82%	94%
This paper ($a=0.05$)	57%	59%

12

13

14 **Table 5:** Change in the wintertime ice coverage (days) from the 1998–1997 period to the 1998–
 15 2007 period, for each column of Lake 1 models with four different combinations of albedo
 16 parameter and adjustable parameters of Table 2. The same sets (a–d) are used in Fig. 14.

Column depth (m)	(a) 0.45, Set 3	(b) 0.05, Set 3	(c) 0.45, Set 4	(d) 0.05, Set 4
50	-27.5	-19.3	-57.6	-33.6
100	-52.8	-33.8	-52.1	-16.4
200	-41.2	-14.7	-15.1	0

17

18

19

20

21

22

23

24

25

26

27

28

29

30

31

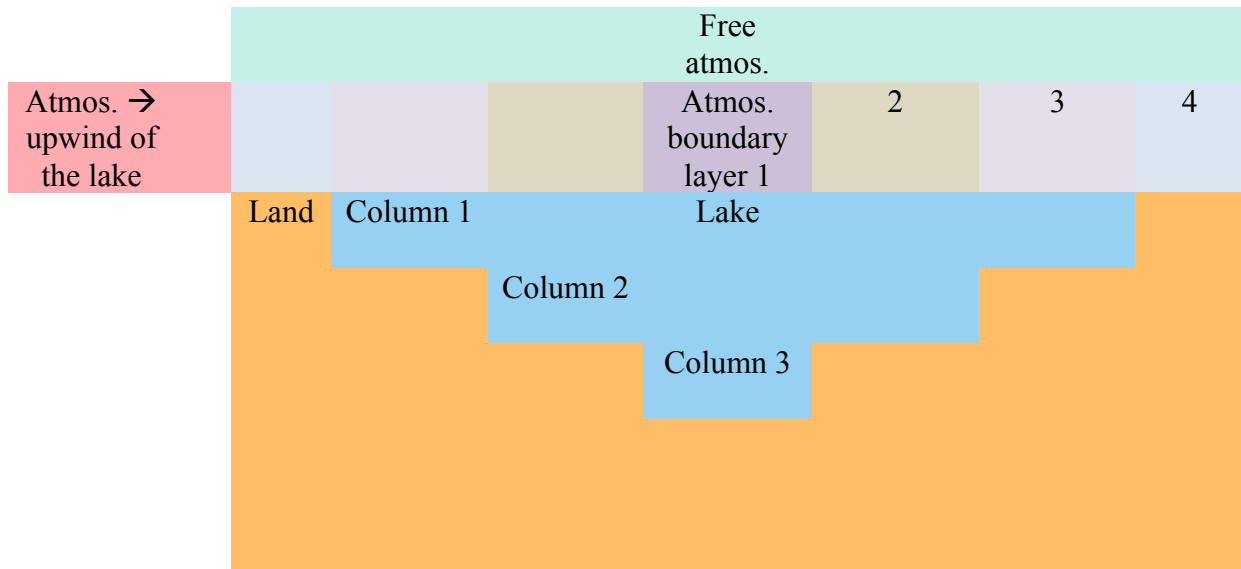
32

33

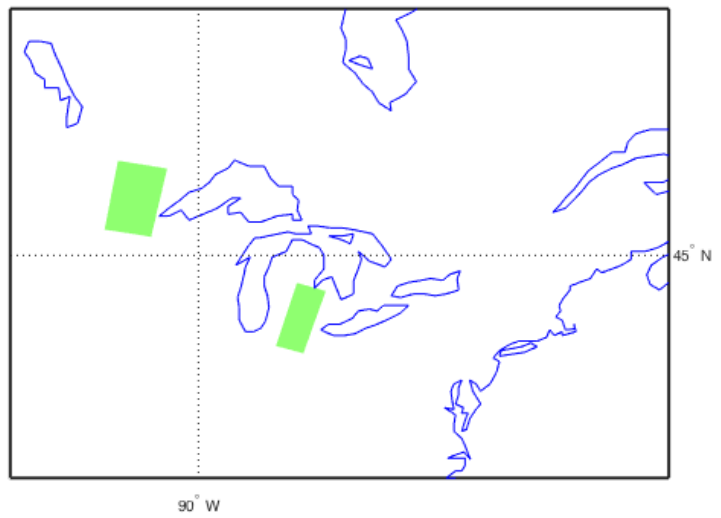
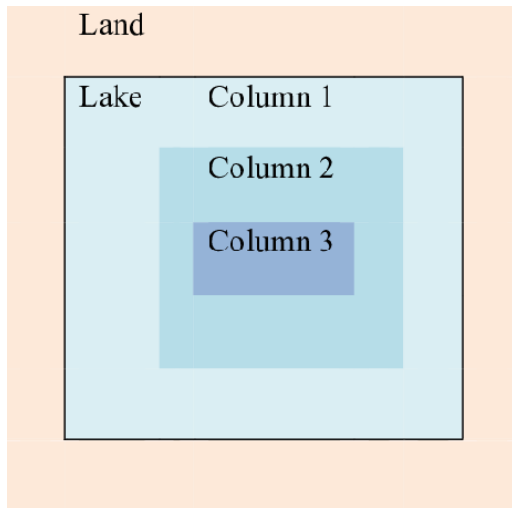
34

35

36

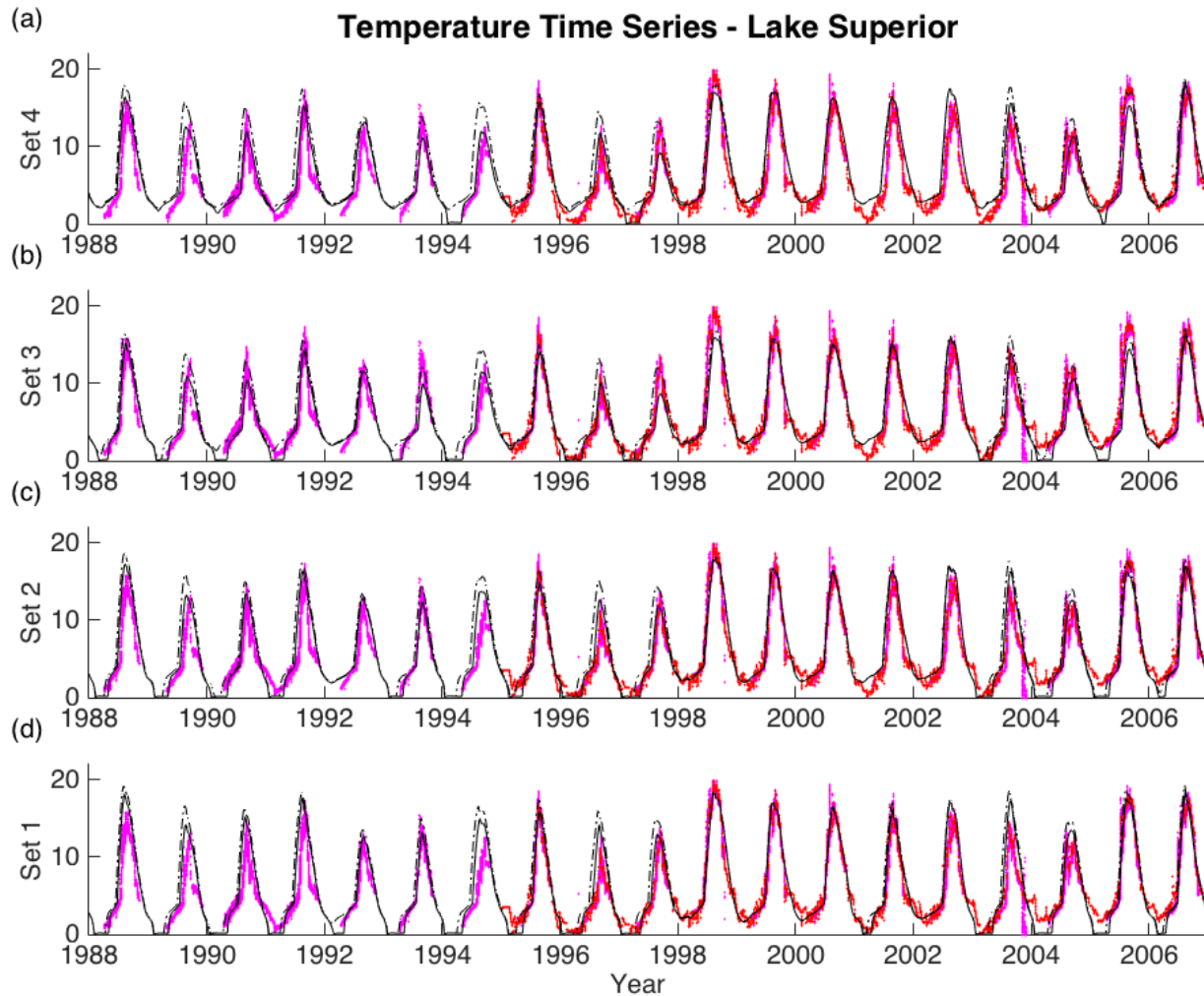


1

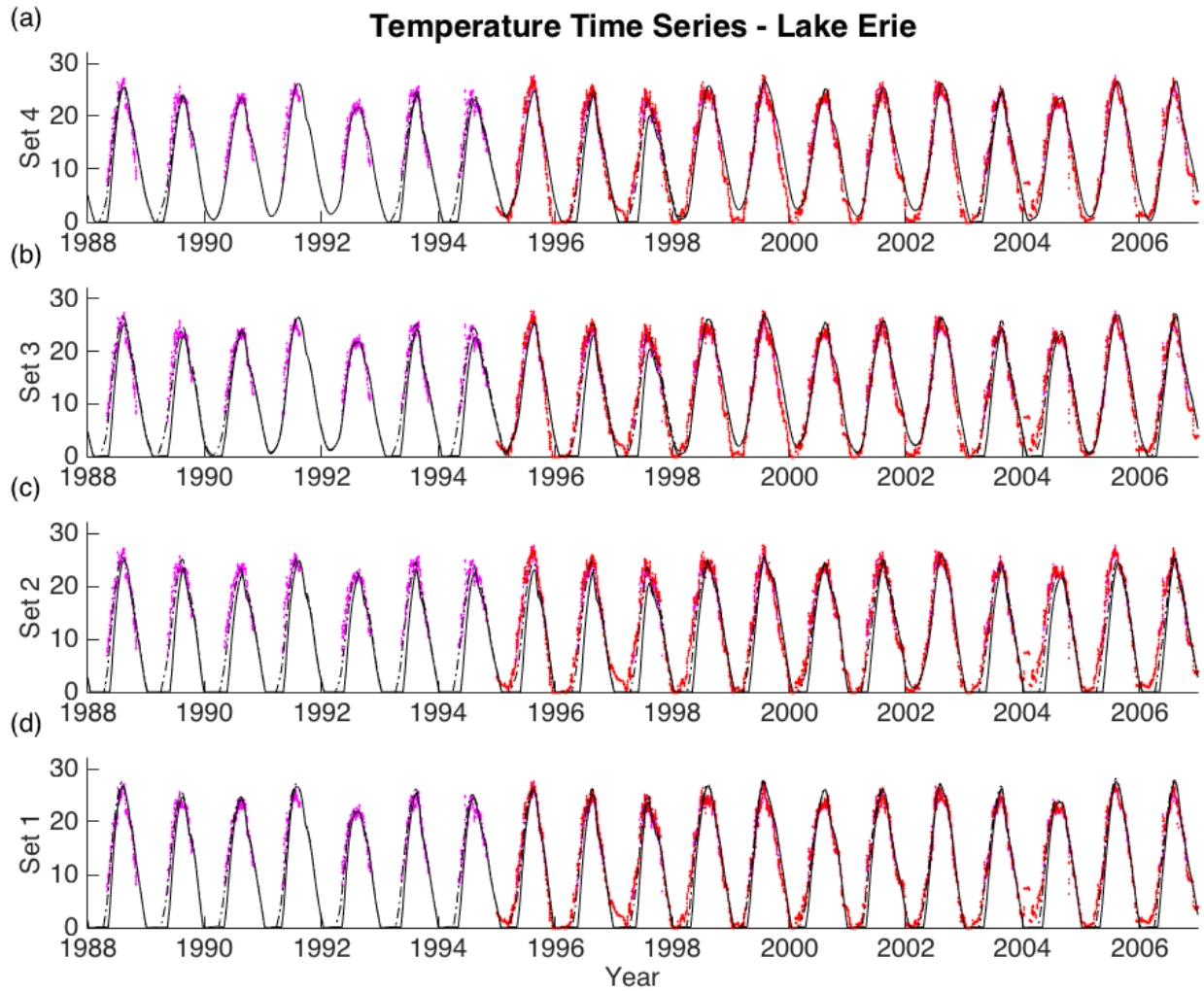


2

3 **Figure 1:** Coupled model geometry. Top: cross-section view; bottom left: plan view. Bottom
 4 right: green shading denotes the regions used to compute upwind forcing temperature $T_{wind}(t)$
 5 [see (1) and section 2.2].



1
 2 **Figure 2:** Observed and simulated time series of daily-mean surface water temperature ($^{\circ}\text{C}$) of
 3 the eastern Lake Superior, with the simulated data coming from the Lake-1 models with (a) Set
 4 Set 4, (b) Set 3, (c) Set 2, and (d) Set 1 parameter sets (Table 2). The purple dots show the observed
 5 surface temperature time series based on the data from the NDBC surface buoy station 45004 in
 6 the eastern Lake Superior (lake depth at this location is 237m). The red dots are daily-mean
 7 surface water temperature at the same location based on the GLSEA data. The simulated surface
 8 temperatures (black) are those over the 200-m column of each lake model considered; solid
 9 curves correspond to model simulations with the lake-ice albedo set to 0.45, and dash-dotted
 10 curves — to the simulations with the lake-ice albedo of 0.05 (dash-dotted curves).



1

2 **Figure 3:** The same as in Fig. 2, but for the surface temperature observations of Lake Erie and
 3 the simulations of Lake-2 model. The NDBC buoy data (purple dots) correspond to the Lake
 4 Erie's buoy station 45005 (lake depth of 10m). The simulated time series shown are those for
 5 surface temperatures over the 15-m column of Lake-2 model.

6

7

8

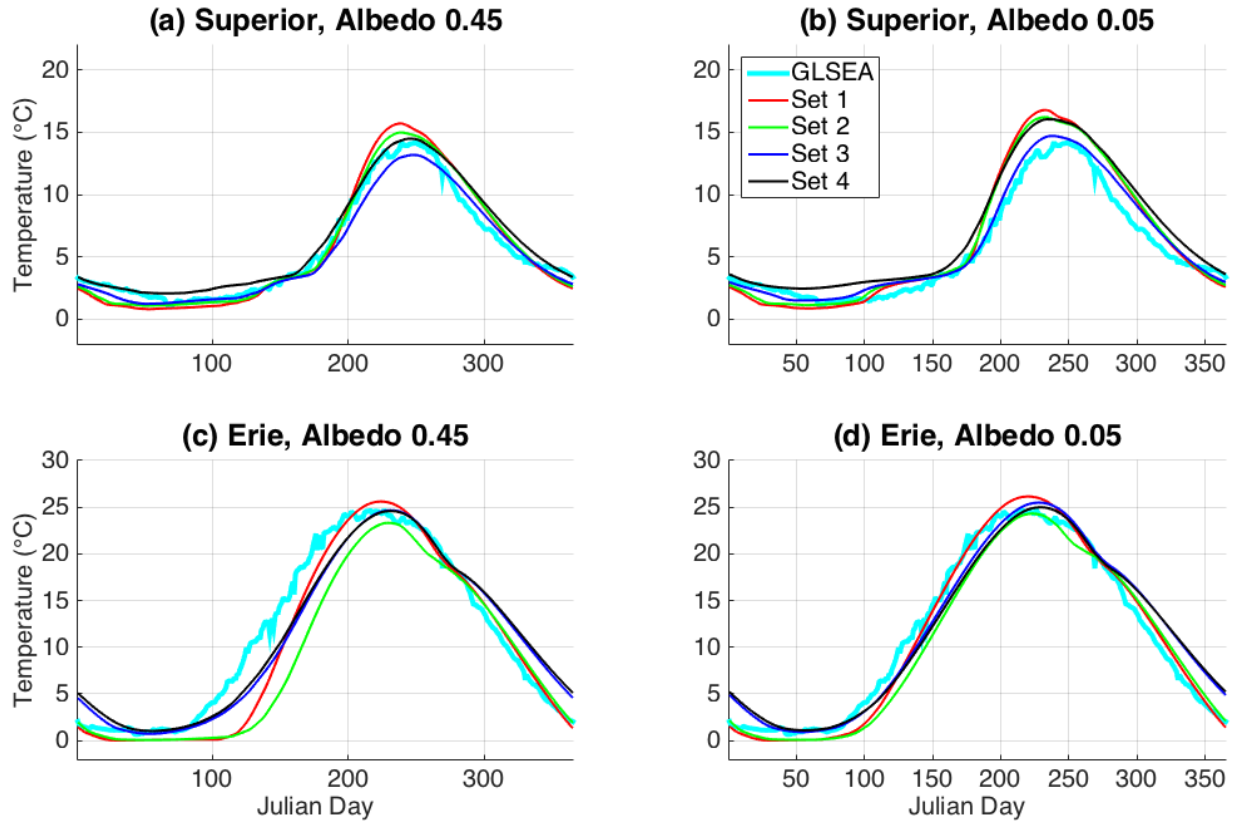
9

10

11

12

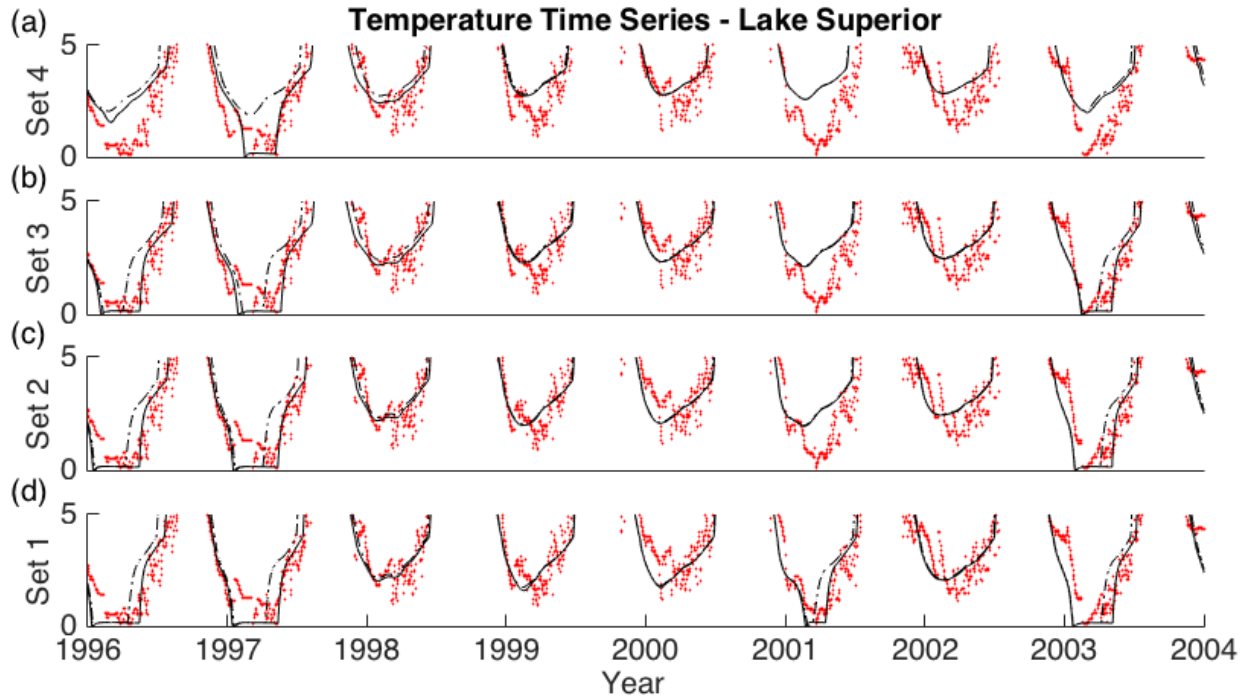
13



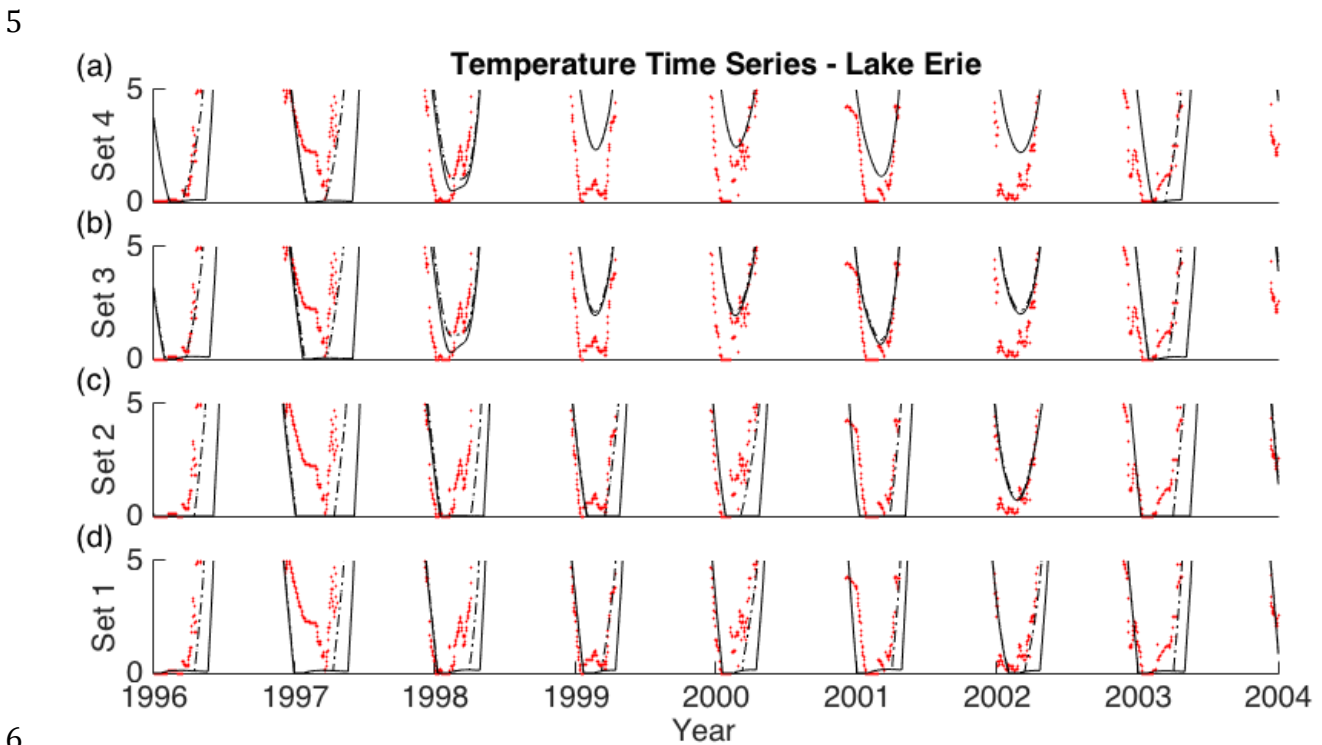
1
2

3 **Figure 4:** The observed and simulated 1995–2005 average seasonal cycles of surface water
 4 temperature based on the data from Figs. 2 and 3. The observed cycles shown here were
 5 computed using the GLSEA data. See panel captions and figure legend to identify the results
 6 from different simulations listed in Table 2. Note that the results displayed here encompass
 7 model simulations both with and without the ice–albedo feedback.

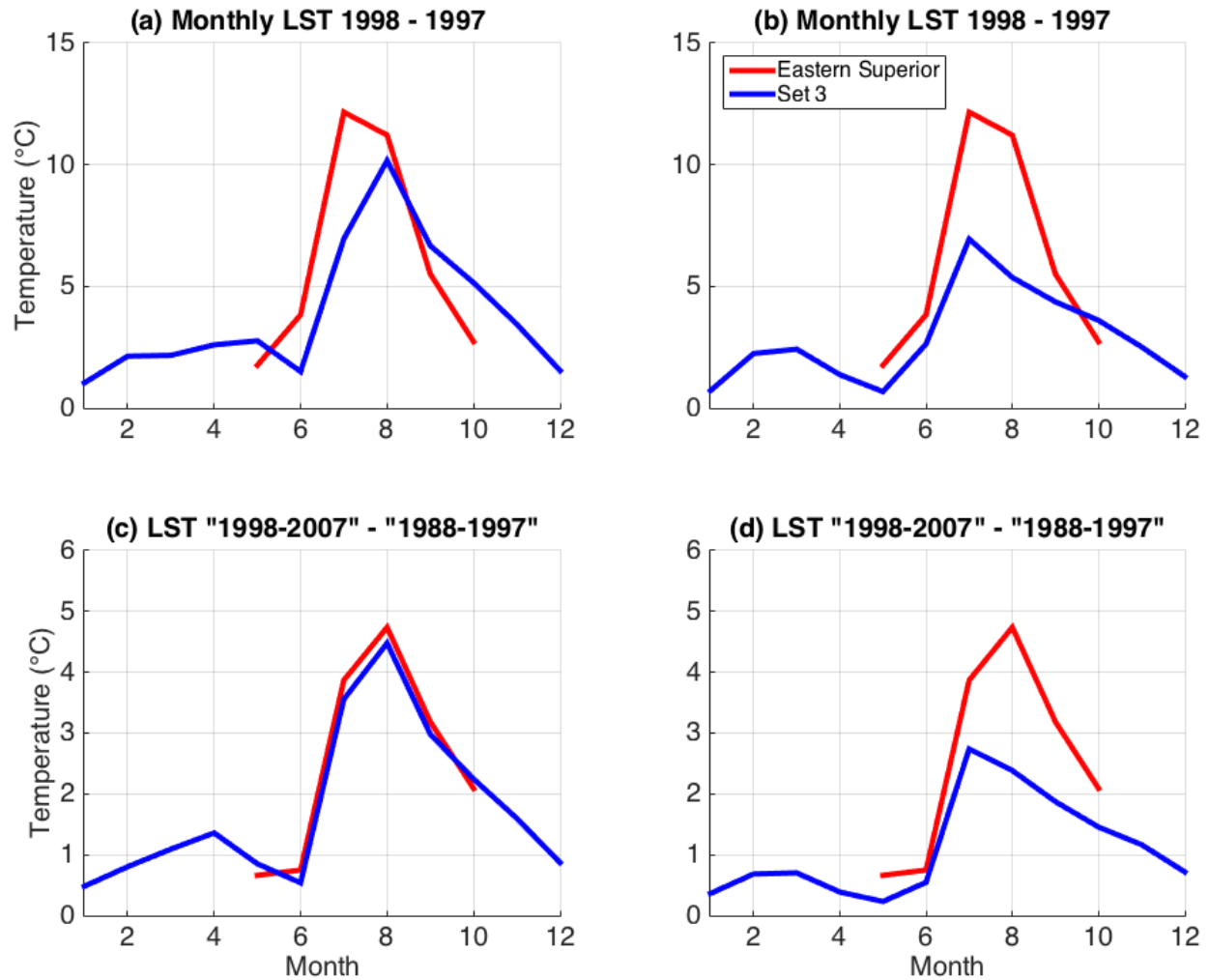
8
9
10
11
12
13
14
15



1
 2 **Figure 5:** The close-up of the surface-temperature time series shown in Fig. 2 (Lake Superior)
 3 restricted to the 1996–2004 period and to the 0–5°C range of lake-surface temperatures to
 4 emphasize the cold-season temperature variability.

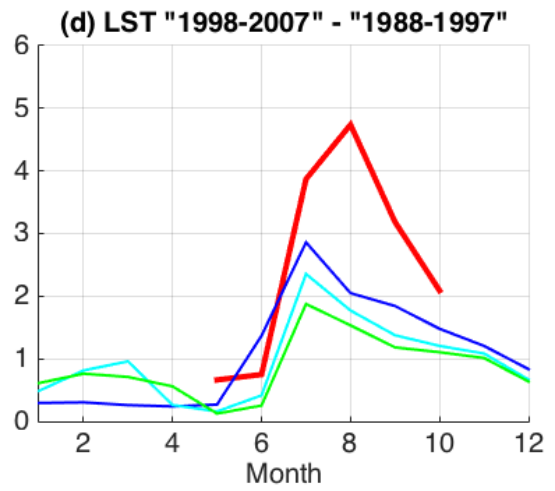
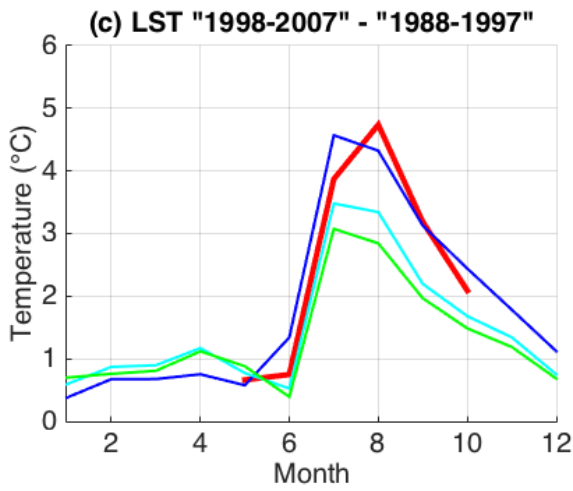
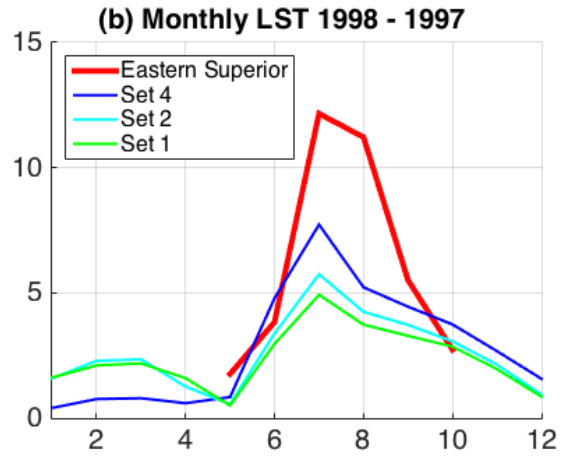
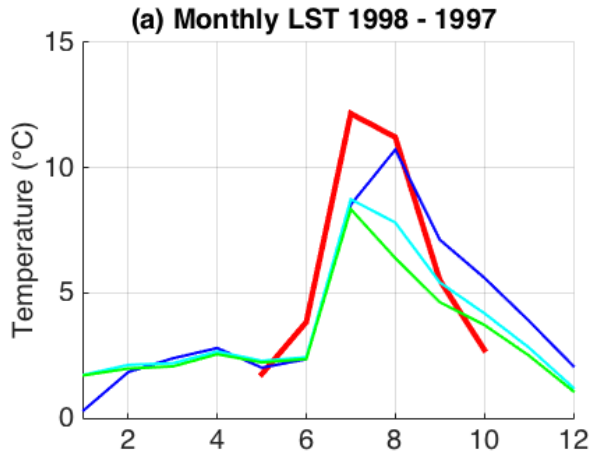


6
 7 **Figure 6:** The same as in Fig. 5, but for the close-up view of the Lake Erie time series of Fig. 3.



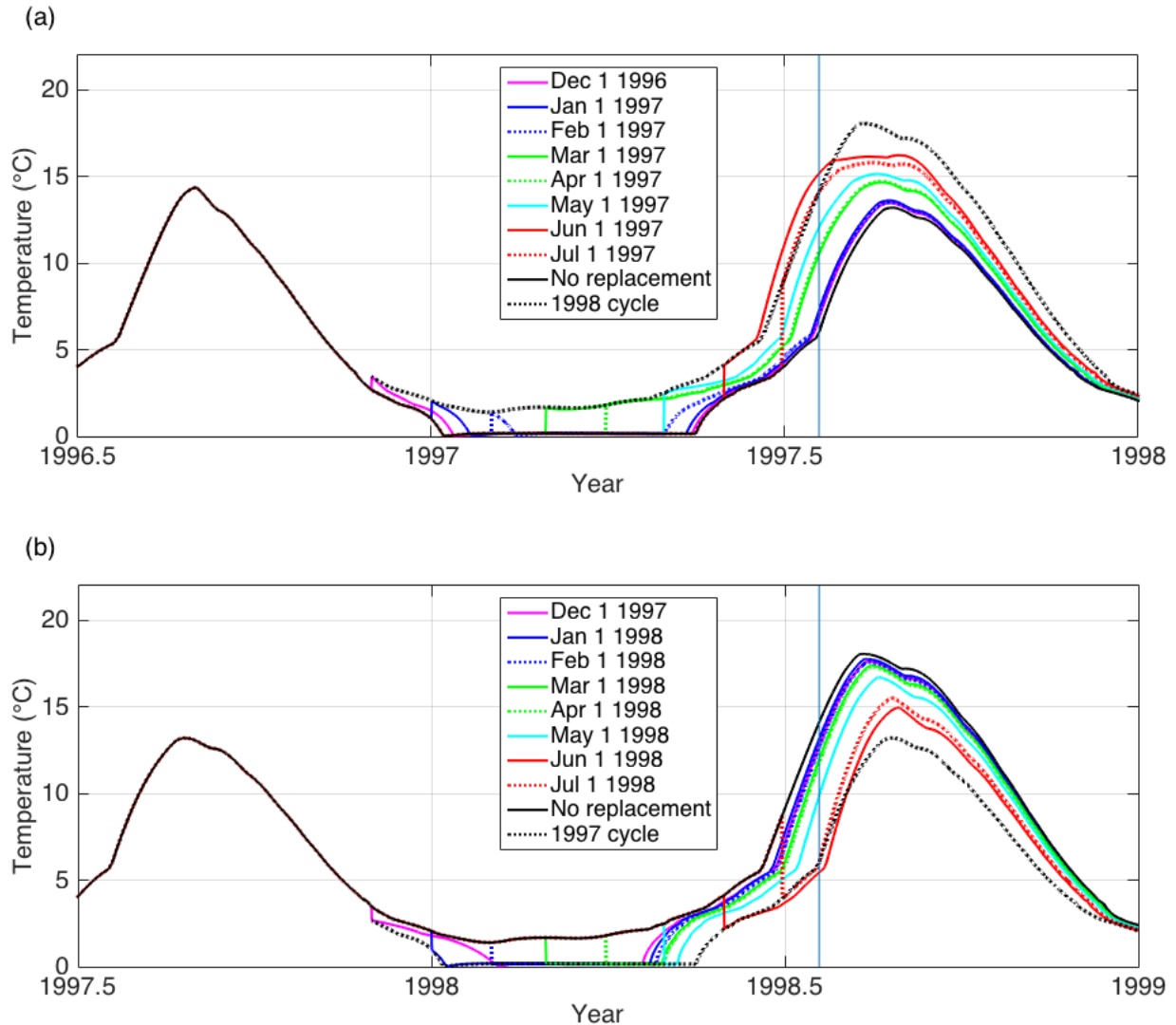
1
2

3 **Figure 7:** The difference in the observed (red) and simulated (blue) seasonal cycle of the eastern
 4 Lake Superior surface temperature between years 1998 and 1997 (top), as well as between the
 5 10-yr-mean seasonal cycle based on 1998–2007 and 1988–1997 decades (bottom). We used
 6 observations of surface temperature for NDBC buoy station 45004 in the eastern Lake Superior
 7 (lake depth of 237m there), and simulations with Lake 1 model with parameter set 3 from see
 8 Table 2; shown here are simulated surface temperatures over the 200-m column of this model.
 9 Left column of the figure: ice albedo was set to the default value of 0.45; left column: ice albedo
 10 was set to the open-water value of 0.05.



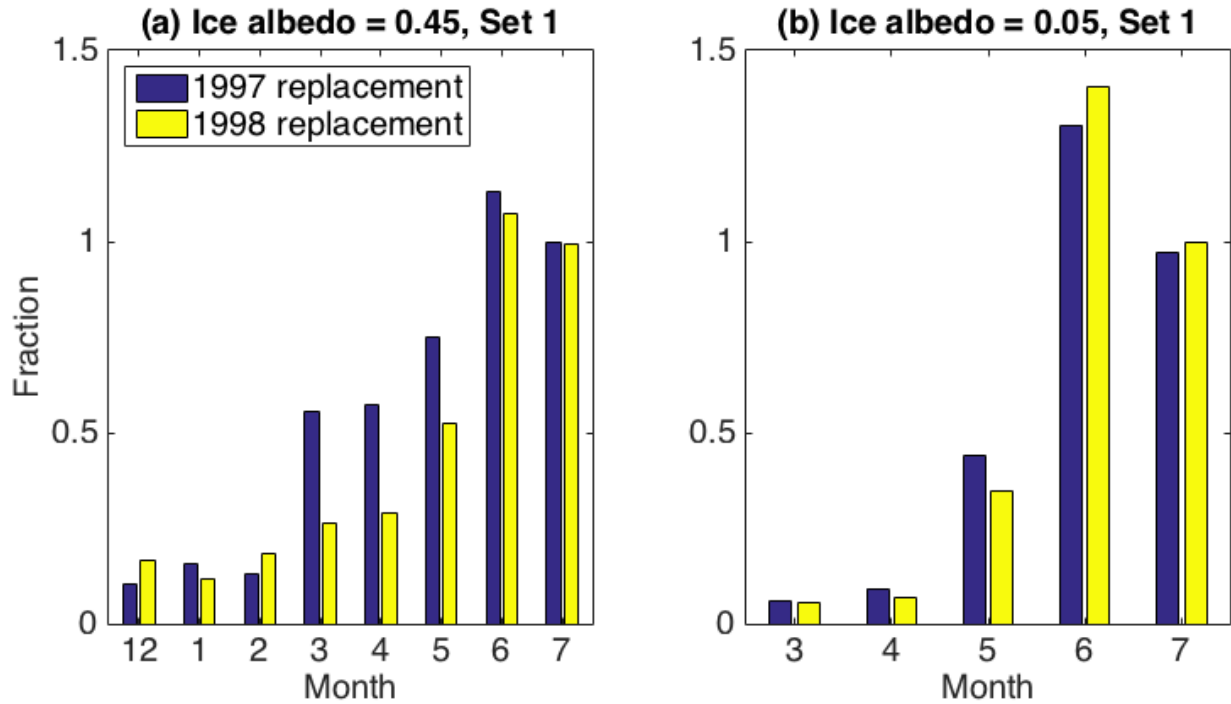
1
2
3
4
5
6
7
8
9
10
11
12
13
14
15
16
17
18

Figure 8: The same as in Fig. 7, but for Lake 1 model simulations using parameter sets 1, 2 and 4 of Table 2 (see figure legend).



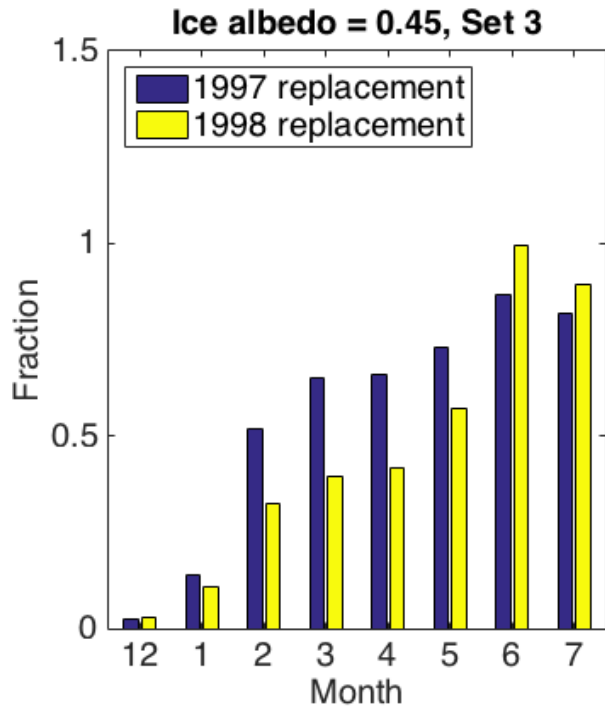
1
 2 **Figure 9:** Initial condition replacement experiments for 1996/97–1997/98 warming simulated by
 3 the Lake 1 model with parameter set 1 of Table 2 and the default ice-albedo value of 0.45. In (a),
 4 solid black curve show the July 1, 1996–December 31, 1998 segment of the simulated lake-
 5 average surface temperature time series. Black dotted curve, on the other hand, shows the
 6 simulated surface temperature evolution shifted backwards by one year, thus corresponding to
 7 the period from December 1, 1997 through December 31, 1998. Different colored lines show the
 8 results of the simulations under the July 1, 1996–December 31, 1998 external forcing, in which
 9 the lake temperature and ice conditions were replaced, on a certain date, by the conditions one
 10 year later; that is, the states reflected by the black solid curve were replaced by the corresponding
 11 states on the black dotted curve. Replacement dates are given in the panel legend. Panel (b)
 12 shows the results of the experiments analogous to those in (a), except the roles of 1997 and 1998
 13 were switched, that is, the 1996/97 initial conditions were used in conjunction with the 1997/98
 14 external forcing history. Vertical line in each panel marks the location of the July 20 date.

15



1
2

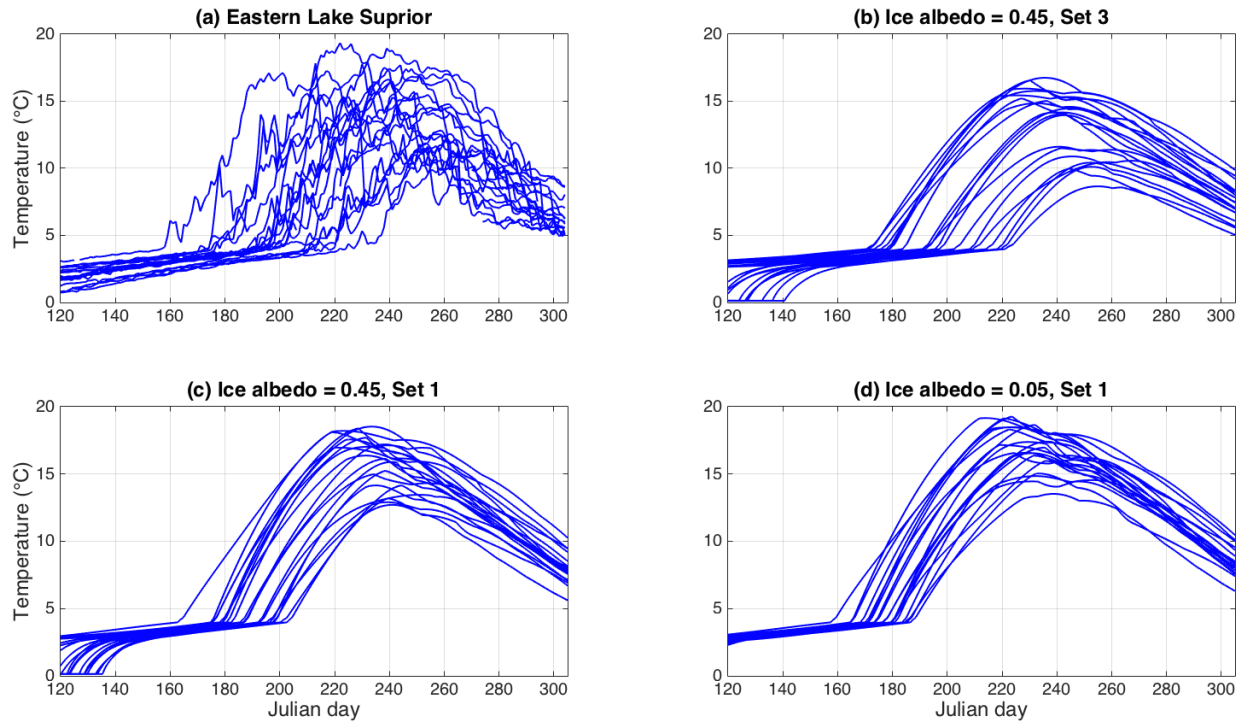
3 **Figure 10:** Role of antecedent lake conditions in the simulated 1997/98 warming of Lake
 4 Superior. Shown is the fraction of the simulated surface temperature difference between July
 5 20, 1997 and July 20, 1998 (this difference peaks on July 20, hence the choice of the date)
 6 realized in the initial condition replacement experiments of Fig. 9. For example, the blue bar
 7 in panel (a) for month 3 measures the ratio of the difference between solid green and black
 8 curves to the difference between dotted black and solid black curves in Fig. 9a, for July 20;
 9 this ratio turns out to approximately equal 0.6: 60% of the full simulated warming thus
 10 reflects lake's memory of the March initial conditions. The yellow bars in panel (a) show the
 11 results based on the 1998 replacement experiments from Fig. 9b. Panel (b) shows analogous
 12 results for the lake model in which the ice–albedo feedback was artificially suppressed. The
 13 ratios shown in (b) still correspond to the July 20 date, as in (a).



1
2

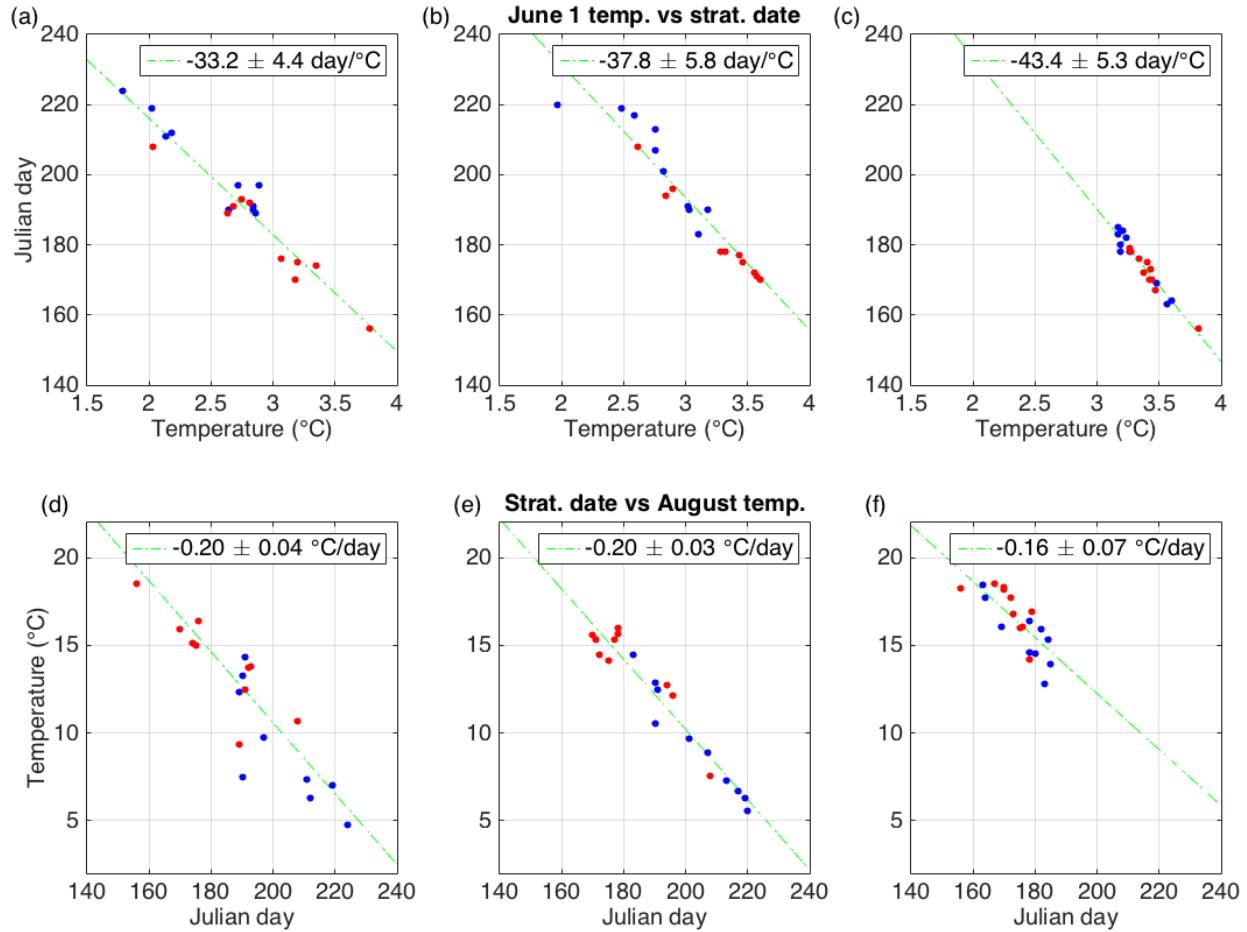
3 **Figure 11:** The same as in Fig. 10a, but for the Lake 1 model with parameter set 3 of Table 2.
 4 The date of maximum summertime temperature difference between 1997 and 1998 on which the
 5 fractions of warming explained by the replacement experiments are recorded in these simulations
 6 is August 8.

7
8
9
10
11
12



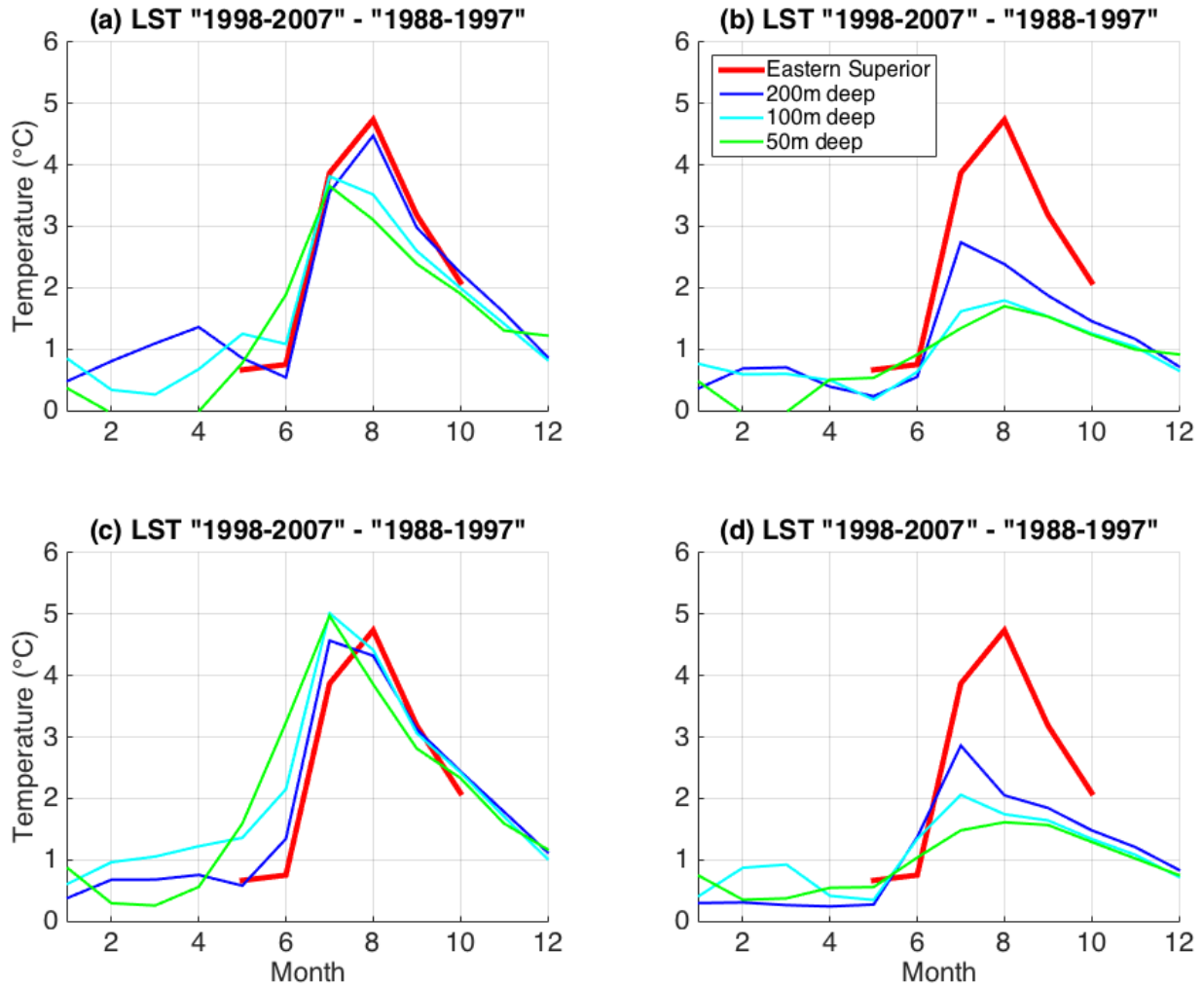
1
2
3
4
5
6
7
8
9
10
11
12

Figure 12: Spaghetti plots of observed and simulated May–October lake-surface temperature time series for each year between 1988 and 2007. (a) Observed temperatures (NDBC’s eastern Lake Superior buoy 45004, depth of 237m); (b, c) Simulated 200-m column surface temperatures for Lake 1 model with parameter sets 3 and 1, respectively (Table 2), and ice albedo of 0.45; (d) The same as in (c), but for the model with the ice albedo set to 0.05.



1
2
3
4
5
6
7
8
9
10
11
12
13
14
15

Figure 13: Connection between the onset of summertime stratification and lake temperatures. (a) Scatter plot of the daily-mean lake-surface temperatures at the NDBC buoy station 45004 in the eastern Lake Superior on June 1 (before the onset of the stratification) versus the start dates of summertime thermal stratification (that is, the date on which daily-mean lake-surface temperature at this location warmed above 3.98°C for the first time after winter). The blue dots correspond to years between 1988 and 1997, and the red dots correspond to years between 1998 and 2007. (b) The same as in (a), but for the surface temperature of 200-m column of Lake 1 model with parameter set 3 of Table 2 and the default ice-albedo value of 0.45; (c) the same as in (b), but for the Lake 1 model with parameter set 1 of Table 2 and the ice-albedo value of 0.05. Panels (d–f) are analogous to (a–c), but document the connection between the onset of stratification and August-mean lake surface temperature (that is, after the onset of summertime stratification); note also that the axes here are flipped with respect to the axes in panels (a–c).



1

2

3 **Figure 14:** The difference between the 10-yr-mean seasonal cycle of the eastern Lake Superior
 4 surface temperature based on 1998–2007 and 1988–1997 decades, in observations and model
 5 simulations. We used observations of surface temperature for NDBC buoy station 45004 in the
 6 eastern Lake Superior (lake depth of 237m there) [red], and simulations of Lake 1 models with
 7 Table 2 parameter sets 3 (top row) and 4 (bottom row). Shown are the simulated surface
 8 temperatures over the 200-m (blue), 100-m (cyan) and 50-m (green) columns of these models.
 9 Left column of the figure: ice albedo in the model was set to the default value of 0.45; right
 10 column: ice albedo was set to the open-water value of 0.05.

11